Streamflow depletion estimation for conjunctive water management in a heavily-stressed aquifer using analytical depletion functions

Samuel C. Zipper[1,*], Tom Gleeson[2,3], Qiang Li[2,3], Ben Kerr[3]
1. Kansas Geological Survey, University of Kansas, Lawrence KS, USA
2. Department of Civil Engineering, University of Victoria, Victoria BC, Canada
3. Foundry Spatial Ltd., Victoria BC, Canada
* samzipper@ku.edu

Author ORCiD IDs:
Zipper: 0000-0002-8735-5757
Gleeson: 0000-0001-9493-7707
Li: 0000-0003-2221-6905
Kerr: NA

This is a non-peer-reviewed manuscript which has been submitted to *Water Resources Research.*

Keywords: analytical models, MODFLOW, water management, decision support, streamflow depletion

Key Points:

- We compared streamflow depletion estimates from analytical depletion functions to a numerical model in a heavily-stressed aquifer.
- Analytical depletion functions had similar estimates of streamflow depletion with lower data and computational costs than numerical models.
- Analytical depletion functions are a potential tool for decision making in settings where numerical models are not available.

Abstract

Groundwater pumping can lead to reductions in streamflow ('streamflow depletion') and estimating streamflow depletion is critical for conjunctive groundwater-surface water management. Streamflow depletion can be quantified using either analytical models, which have low data requirements but many simplifying assumptions, or numerical models, which represent physical processes more realistically but have high data, effort, and expertise requirements. Analytical depletion functions are a recently-developed tool that address some of the limitations of analytical models, but to date have only been evaluated under relatively simple conditions. Here, we evaluate eight different analytical depletion functions across a range of groundwater abstraction, physiographic, and hydrostratigraphic conditions via comparison to the Republican River Compact Administration groundwater model, a calibrated MODFLOW numerical model used for conjunctive water management in a heavily-stressed portion of the High Plains Aquifer (USA). We find mostly strong agreement between the analytical depletion functions and the MODFLOW model, though analytical depletion functions underestimate depletion for wells close to surface water features in high transmissivity environments. Compared to previous work, there is little variability among the eight analytical depletion functions, indicating that function formulation plays a minor role in this setting. Analytical depletion function performance is strongly influenced by hydrostratigraphic parameters (storativity and transmissivity) but performance is insensitive to pumping rate, confirming a key assumption of analytical models. Overall, analytical depletion functions provide comparable estimates of streamflow depletion to numerical models at a fraction of the time and data requirements. Accurate hydrostratigraphic data are essential to estimating streamflow depletion regardless of modeling approach.

Plain Language Summary

Estimating the impacts of groundwater pumping on streamflow ('streamflow depletion') is challenging but essential for effectively managing water resources. In this study, we test a low-cost, low-effort approach (called an 'analytical depletion function') to estimate streamflow depletion by comparing it to a more complex tool that is currently used for water management in a heavily-irrigated setting in the central US. We find that there is general agreement between the analytical depletion function and the more complex approach. We also test whether analytical depletion function performance is better or worse for different conditions, and find that performance is similar regardless of pumping rate but very sensitive to properties of the subsurface. Overall, our results indicate that analytical depletion functions could be useful tools for estimating streamflow depletion where more complex approaches are unavailable, but having accurate data about the subsurface is essential.

1 Introduction

Groundwater is an essential contributor to streamflow around the world (Beck et al. 2013), providing a relatively cool and stable supply of water particularly during dry periods.

Groundwater inflow to streams (‘baseflow’) is essential for a number of aquatic and groundwater-dependent ecosystems (Rohde et al. 2017; Larsen and Woelfle-Erskine 2018). However, groundwater abstractions can lead to reductions in streamflow (‘streamflow depletion’) via the capture of discharge, which includes interception of water which otherwise would have discharged into a stream or, in extreme cases, induced infiltration from a previously gaining stream (Bredehoeft et al. 1982; Bredehoeft 2002; Barlow et al. 2018).

Streamflow depletion cannot be directly observed and is often difficult to estimate due to complex groundwater flow systems, lag times between pumping and streamflow reductions, and natural variability in streamflow resulting from other processes such as weather, water control structures such as dams, and surface water withdrawals (Barlow and Leake 2012). For this reason, conjunctive groundwater-surface water management typically relies on numerical models (e.g. MODFLOW), which are physics-based simulations of groundwater flow processes (McDonald and Harbaugh 1988; Fienen et al. 2018). However, there are large time, effort, and computational costs associated with numerical models (Fienen et al. 2015, 2016). They are, therefore, not available in most settings.

In locations where numerical models are not available, analytical models are often used instead (Hamilton and Seelbach 2011; Huang et al. 2018). Analytical models are simpler representations of stream-aquifer interactions, but contain many limiting assumptions such as one (or occasionally two) streams, homogeneous subsurface conditions, and simplified stream and aquifer geometry. While analytical models have been proposed that account for some of these assumptions (Butler et al. 2007; Yeh et al. 2008; Zlotnik and Tartakovsky 2008; Singh 2009), there are still many real-world environments which violate the core assumptions of analytical models including settings where there are multiple and/or highly sinuous streams.

Recently, analytical depletion functions (Figure 1) have been proposed as a potential extension of existing analytical models which empirically address some of these limitations for use in complex, real-world settings (Zipper et al. 2019b). An analytical depletion function consists of (i) *stream proximity criteria*, which identify the streams that may be affected by a well; (ii) a *depletion apportionment equation*, which calculates how depletion from a single well should be allocated to multiple stream segments meeting the stream proximity criteria; and (iii) an *analytical model*, which estimates depletion in each stream segment meeting the proximity criteria.

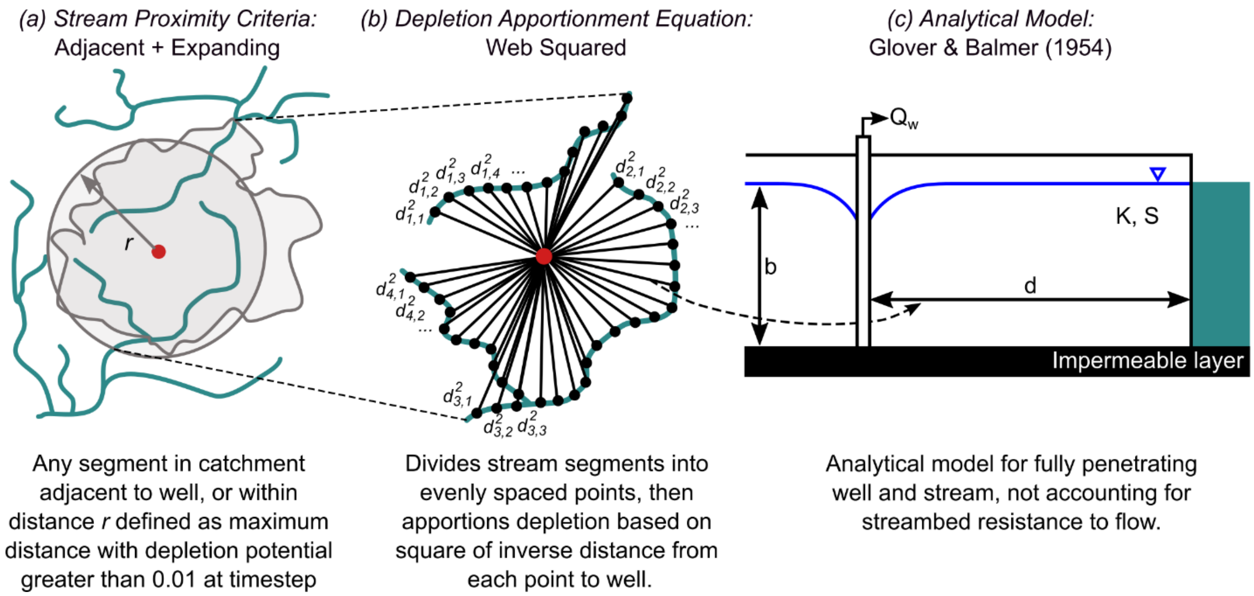

Figure 1. Components of an analytical depletion function. Modified from Zipper et al. (2019a) under CC-BY 3.0 license.

Analytical depletion functions have only been subjected to limited testing in a small number of study sites. During the development of the State of Michigan's Water Withdrawal Assessment Tool, Reeves et al. (2009) compared nine different depletion apportionment equations for a small watershed in Michigan and found that an inverse distance-based approach best matched output from a MODFLOW numerical model. Subsequently, Zipper et al. (2018a) evaluated five depletion apportionment equations for several real-world stream networks in British Columbia, finding that a new inverse distance-based approach which considers stream geometry (called web squared; Figure 1b) performed the best under steady-state conditions. Zipper et al. (2019b) introduced the concept of stream proximity criteria (Figure 1a) and performed a sensitivity analysis to 50 combinations of stream proximity criteria, depletion apportionment equation, and analytical model, finding that analytical depletion functions were able to accurately estimate the distribution and magnitude of streams affected by a well. However, Zipper et al. (2019b) compared analytical depletion functions to an archetypal numerical model with several simplifications including a homogeneous subsurface and stream properties. Li et al. (2020) conducted the first comparison of analytical depletion functions to a calibrated numerical model, but this was in unstressed conditions with only a single well pumping at any given time and did not evaluate different analytical depletion function formulations.

As a result, it remains unknown whether analytical depletion functions are suitable tools for heavily-stressed aquifers with significant ongoing pumping, particularly since evidence indicates that cumulative impacts of multiple wells may not be linearly additive (Ahlfeld et al. 2016). Further, the degree to which well and hydrostratigraphic characteristics influence the performance of analytical depletion functions has not been previously evaluated. Thus, the ability of analytical depletion functions to predict streamflow depletion in complex, heterogeneous, and highly-stressed real-world settings where cumulative impacts of multiple wells are occurring simultaneously remains unknown. In this study, we address this knowledge gap by comparing a suite of analytical depletion functions to a complex, calibrated groundwater model of the Republican River Basin (USA) which is currently used for conjunctive water management (RRCA 2003). Specifically, we ask:

(1) Do analytical depletion functions estimates of streamflow depletion in a complex, highly-stressed, unconfined aquifer agree with an existing calibrated numerical model?

(2) How does agreement between analytical depletion functions and the numerical model vary as a function of formulation, hydrogeological properties, stream properties, landscape attributes, and time of year?

2 Methods

2.1 Republican River Compact Administration groundwater model

The Republican River Watershed drains approximately 64,500 km^2 (24,900 mi^2) of the US High Plains, flowing through Colorado, Nebraska, and Kansas (RRCA 2003). There is significant irrigated agriculture within the watershed (Deines et al. 2017, 2019) and, as a result, the surface and groundwater resources in the Republican River Watershed and surrounding High Plains Aquifer are heavily stressed (Haacker et al. 2016; Butler et al. 2018). To allocate and manage the water of the Republican River, the three states entered into the Republican River Compact in 1942 (Khan and Brown 2019). Following a US Supreme Court decision in 2002, representatives from Kansas, Nebraska, Colorado, the US Bureau of Reclamation, and the US Geological Survey collaboratively constructed the Republican River Compact Administration (RRCA) groundwater model as a tool for quantifying streamflow depletion caused by groundwater pumping. The model is updated annually to guide water allocations among the three states. The model is described in detail in RRCA (2003) and all model files are available on the Republican River Compact Administration website (https://www.republicanrivercompact.org/).

The RRCA model spans an area larger than the Republican River watershed and is bounded by the Platte River in the north and outcrops of the High Plains Aquifer on the east, west, and south. The model is constructed using MODFLOW-2000 (Harbaugh et al. 2000) covering a total active domain of 77,868 km^2 (30,065 mi^2), which is discretized into 2.6 km^2 (1 mi^2) grid cells. The model is updated annually with each year's estimated pumping data submitted by each state. Here, we use version 12p, which is the version originally released that spans the period 1918-2000 at a monthly timestep. While the High Plains Aquifer in this region is unconfined, the RRCA model adopts an assumption of constant transmissivity to improve model stability. In MODFLOW-2000, constant transmissivity in transient simulations requires that the aquifer is parameterized as confined and, as a result, requires specific storage as model input rather than specific yield. To appropriately represent unconfined aquifer storage properties with a confined parameterization, the RRCA calculates specific storage for each grid cell as the estimated specific yield divided by saturated thickness in each grid cell (RRCA 2005).

The model represents surface water features using a combination of three MODFLOW packages (Figure 2; Figure S1): the stream package (STR), which is used for the Republican River and tributaries and allows stream cells to dry in response to pumping; constant head boundaries (CHB), which are used for the Platte River at the north edge and the eastern edge of the model; and the drain package (DRN), which represent springs and are primarily along the southeastern portion of the domain. Direct uptake of groundwater by phreatophytes is represented using the evapotranspiration (EVT) package, and primarily occurs in cells along stream channels with shallow groundwater. There are a total of 9372 pumping wells in the domain, each of which has a monthly pumping schedule which primarily occurs during the June-September growing season (Figure S2; Figure S3).

The model was calibrated via comparison to groundwater levels (350,233 records from 10,835 locations) and baseflow (65 records) for the historical pumped period. Hydraulic conductivity and precipitation recharge rates were the primary calibration parameters. Since the calibration period included the expansion of pumping across the watershed, calibrating to baseflow across the historic period provides confidence that the model is able to simulate the response of groundwater-surface water interactions in response to groundwater pumping. Complete calibration results are available at the RRCA website for baseflow (https://www.republicanrivercompact.org/v12p/html/ch07.html) and groundwater levels (https://www.republicanrivercompact.org/v12p/html/ch08.html). Since baseflow is the more relevant calibration target for our investigation, we included several calibration scatterplots in the supplemental information (Figure S4, S5, S6). There tends to be more variability in performance in smaller tributaries compared to the Republican River main stem. During model development, fit between observations and predictions was evaluated by experts from the model development team, which was made up of representatives from each of the affected states and the federal government, and deemed to be acceptable for water allocation decisions related to streamflow depletion (RRCA, 2003).

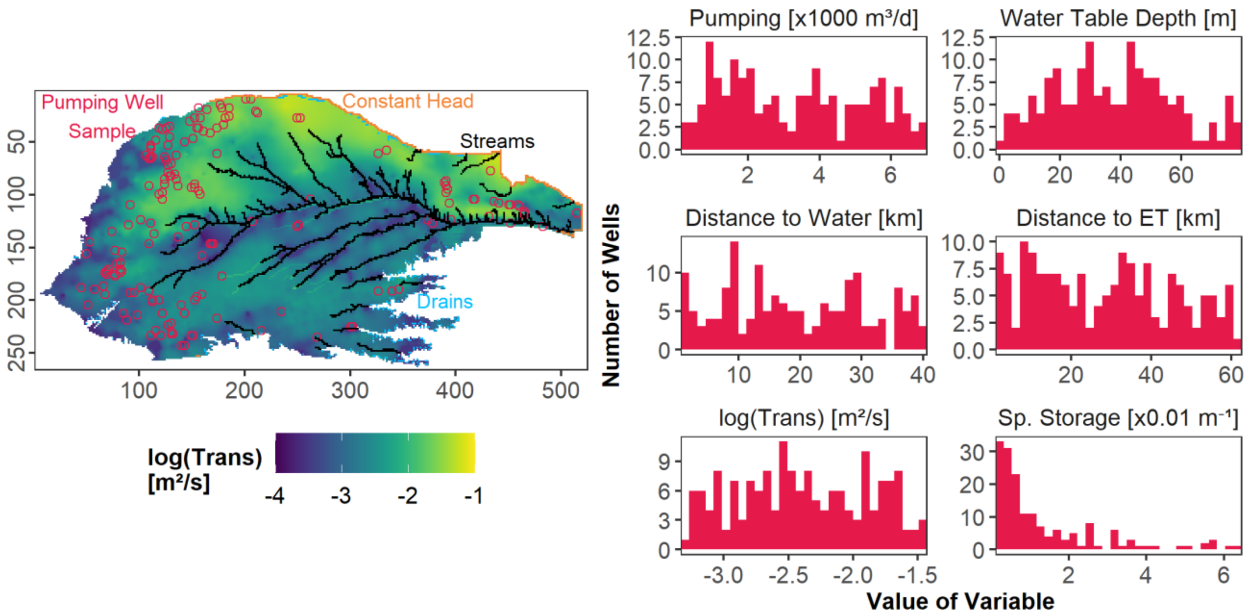

Figure 2. (left) Map showing Republican River Compact Administration MODFLOW model domain, hydrostratigraphic properties, and selected pumping wells for pumping experiment. (right) Properties of wells sampled for pumping experiment, which are described in detail in Section 2.3.1 of the text.

2.2 Analytical depletion functions

Analytical depletion functions are described in detail in Zipper et al. (2019b), so only a brief overview is presented here. Analytical depletion functions consist of three components (Figure 1):

(i) stream proximity criteria, which identify the stream segments that may be depleted by a well as a subset of the total stream network;

(ii) a depletion apportionment equation, which calculates the fraction (f_i) of the well's total depletion that is sourced from each stream segment (i) meeting the stream proximity criteria. For each well, f_i of all stream segments must sum to 1.0; and

(iii) an analytical model, which calculates the streamflow depletion for each stream segment without considering other stream segments (Qa_i). The calculation of Qa_i follows the typical use of analytical models which assume infinite stream length.

For that well, the estimated volumetric streamflow depletion in each segment, Qs_i, is then calculated as, $Qs_i = f_i * Qa_i$.

The inclusion of stream proximity criteria and depletion apportionment equations in analytical depletion functions are intended to empirically account for two major limitations of analytical models: typically analytical models only include one or a limited number of streams, and do not address stream sinuosity. Depletion apportionment equations that subdivide stream segments into multiple points, such as the web and web squared approaches developed by Zipper et al. (2018a), approximate the integral of streamflow depletion along a stream segment of finite length, which addresses the problematic analytical assumption of infinite stream length (Kollet et al., 2002). However, analytical depletion functions still include many of the assumptions of analytical models, including that pumping does not change in recharge and therefore all pumped water is sourced from either groundwater depletion or streamflow depletion. In settings where recharge is unaffected by pumping, the spatial distribution of recharge does not influence the streamflow depletion (Barlow & Leake, 2012; Bredehoeft et al. 1982; Bredehoeft 2002; Feinstein et al., 2016).

Numerous options exist for stream proximity criteria, depletion apportionment equations, and analytical models. These components were systematically evaluated in Zipper et al. (2019b) via comparison to an uncalibrated numerical model of the Navarro River Watershed (California, USA). Zipper et al. (2019b) found that analytical depletion function performance was most sensitive to the choice of depletion apportionment equation, secondarily sensitive to the choice of stream proximity criteria, and relatively insensitive to the choice of analytical model.

In this study, we will compare a subset of 8 of the 50 combinations evaluated by Zipper et al. (2019b). Since Zipper et al. (2019b) found the greatest sensitivity of model performance to the choice of depletion apportionment equation, we compared four unique but related depletion apportionment equations here: web and web squared, which were the two best-performing equations for the Navarro River Watershed, CA (Zipper et al. 2019b); and inverse distance and inverse distance squared, the former of which was the best-performing equation for the Kalamazoo Valley, MI (Reeves et al. 2009). All four depletion apportionment equations can be expressed as:

$$f_i = \frac{\sum_{p=1,P_i} \frac{1}{d_{i,p}^{w}}}{\sum_{j=1,n}\left(\sum_{p=1,P_j} \frac{1}{d_{j,p}^{w}}\right)} \qquad \text{\{Eq. 1\}}$$

The result, f_i is the fraction of total depletion occurring in stream segment *i*. Required inputs include *d*, the distance from the well to the stream segment; *w*, a weighting factor that is equal to 1 for inverse distance and web and equal to 2 for inverse distance squared and web squared; *n* is the total number of affected stream segments identified by the stream proximity criteria (turquoise lines in Figure 1b); and *P* is the number of points each stream segment is divided into (black dots in Figure 1b). The inverse distance and inverse distance squared methods are simplified formulations of Eq. 1 where only the closest point to the well on each stream segment is used and therefore $P = 1$.

Since stream proximity criteria were of secondary importance, we compared two stream proximity criteria: adjacent catchments only, which was used by Reeves et al. (2009), and adjacent+expanding, which Zipper et al. (2019b) found worked best in the Navarro River Watershed. The adjacent+expanding methods includes both adjacent catchments to the well and any catchments in which the estimated streamflow depletion would be greater than or equal to 1% of the pumping rate at a given timestep. As a result, the number of stream segments meeting the stream proximity criteria increases over time.

We tested a single, relatively simple Glover and Balmer (1954) analytical model (herein referred to as the Glover model; Eq. 2):

$$Qa = Qw * \text{erfc}\left(\sqrt{\frac{Sd^2}{4Tt}}\right) \quad \text{\{Eq. 2\}}$$

In Eq. 2, *Qw* is the pumping rate of the well; *S* is the storativity, typically specific yield or specific storage; *T* is the transmissivity; and *t* is the time since pumping began. To account for monthly variation in *Qw*, we used standard superposition techniques to turn the wells on and off (Jenkins 1968). The Glover model contains numerous simplifying assumptions which are violated in the RRCA domain, including a stream fully penetrating to the bottom of the aquifer, a single linear stream, an aquifer of infinite extent extending away from the stream, and no changes in transmissivity in response to pumping. Since Zipper et al. (2019b) found minimal sensitivity to the choice of analytical model and the RRCA MODFLOW model represents surface water using a mixture of packages, some of which do not include streambed conductance as an input which is required for more complex analytical models such as Hunt (1999), we did not test multiple analytical models in this study. However, many analytical models exist with different formulations (reviewed in Huang et al. 2018) and in other hydrogeological settings, different analytical models may be appropriate.

2.3 Analytical depletion function performance evaluation

2.3.1 Selecting pumping well sample

The goal of our study is to examine the performance of analytical depletion functions relative to a MODFLOW model over a range of hydrogeological and physiographic characteristics. Therefore, we selected a subset of 166 wells (of 9372 total pumping wells in the domain) based on the following characteristics: (i) the mean pumping rate, (ii) pre-development water table depth from MODFLOW steady-state output, (iii) the transmissivity of the MODFLOW cell containing the well (log-transformed), (iv) the storativity of the MODFLOW cell containing the well, (v) the distance from the well to the closest surface water feature (active STR, DRN, or CHB grid cell), and (vi) the distance from the well to the closest cell with potential phreatophytic ET (active EVT cell). The distribution of these properties among our experimental sample is shown in Figure 2 and the distribution among all wells is shown in Figure S7. To span each of these characteristics as uniformly as possible, we used the Latin Hypercube Sampling method (McKay et al. 1979) to randomly sample 250 parameter combinations spanning these six characteristics (Zipper et al. 2018b). We then selected the pumping well that had the shortest euclidean distance in parameter space to each parameter sample, resulting in a total of 166 unique pumping wells in our final evaluation because some wells were closest to multiple samples. Several of the selected wells are spatially close to each other because they are in locations that have relatively rare parameter conditions within the multi-dimensional parameter space, such as high specific storage (Figure S7), and therefore multiple nearby wells were selected to effectively sample a wide range of parameter combinations.

2.3.2 Calculating streamflow depletion in MODFLOW model

To calculate the streamflow depletion associated with each of these pumping wells in the MODFLOW model, we first ran a baseline RRCA simulation to calculate the stream-aquifer flux under baseline conditions for each cell containing a surface water feature. The cell-resolution stream-aquifer fluxes were then aggregated to net stream-aquifer fluxes for each stream segment, which were defined (for the STR package) or manually delineated based on stream network geometry (for the DRN and CHB packages). Since many of the DRN cells were discontinuous (Figure 2) and represent springs or seeps rather than stream channels, each DRN segment was delineated as a cluster of nearby DRN cells. To evaluate the sensitivity of the calculated performance metrics to the inclusion of these features, we performed analytical depletion function calculations both including and excluding DRN cells. We then turned off each of the selected wells one-at-a-time for 166 unique numerical experiments (which we refer to as 'pumping simulations' herein) and calculated the net stream-aquifer flux for each stream segments in each pumping simulation. Turning off each well one-at-a-time and comparing to the baseline simulation isolates the amount of streamflow depletion caused by that specific well. Quantitatively, the decrease in stream-aquifer flux in the baseline simulation relative to a pumping simulation is equal to the streamflow depletion caused by that pumping well (and potential numerical model error), and therefore we can calculate streamflow depletion in each segment and at each stress period for each of our 166 pumping wells. We automated MODFLOW runs using the FloPy package for Python (Bakker et al. 2016, 2018).

Since changing groundwater model boundary conditions (such as pumping rates) can impact model convergence and stability, we screened MODFLOW output for anomalous results prior to comparison. We used two approaches to screen for anomalous results in all MODFLOW simulations, each of which corresponds to a single pumping well. First, we identified additive outliers in the timeseries of the difference in overall mass balance error between the pumping simulation and the baseline simulation (Chen and Liu 1993; López-de-Lacalle 2019). Second, we identified any stress period where MODFLOW estimated negative streamflow depletion either in an individual segment or summed across all segments exceeding 1% of the maximum pumping rate for that well. For both of these comparisons, we identified the stress periods at which anomalous MODFLOW results occurred and limited our comparison to the time period between the onset of pumping and the stress period prior to the first anomalous MODFLOW mass balance change (Figure S8). Mass balance outliers indicating convergence issues were identified for 31 of the 166 pumping experiments tested, occurring as early as the 499th stress period and as late as the final (996th) stress period and stress periods with anomalous results from these 31 pumping simulations were removed from analysis as described above. For all other pumping experiments, our comparison was conducted between the onset of pumping and the end of the model simulation period (December 2000).

2.3.3 Calculating streamflow depletion with analytical depletion functions

Input for the analytical depletion functions (the formulations of which are described in Section 2.1) was extracted directly from the RRCA MODFLOW model, described in Section 2.1. Using consistent parameters between the two approaches was intended to focus our comparison on the impact of the simplifications of analytical depletion functions relative to the numerical model on predicted streamflow depletion, since we do not do a direct comparison to field observations of streamflow depletion. The pumping rate (*Qw*) was extracted from the MODFLOW WEL package (Figure S3), with each grid cell representing a unique pumping well. The well-stream geometry (*d*) was extracted as the distance from each well to each grid cell with a STR, CHB, and DRN cell, which were grouped into the same segments used by the MODFLOW model which are described in Section 2.3.2. Due to the discretization of the MODFLOW model, the point spacing for the discretization of segments in the web and web squared depletion apportionment equations was 2.6 km^2 (1 mi^2). Effective transmissivity (*T*) and storativity (*S*) were calculated as the average *T* and *S* for all MODFLOW cells intersected by a straight line between the well and each stream segment. For *S*, we used specific yield, rather than specific storage, as input to the analytical depletion functions because the use of specific storage in the RRCA model is an artifact of model design, as described in Section 2.1. However, as an experiment to test the importance of the storativity approach, we also ran a set of analytical depletion function calculations using specific storage from the MODFLOW model. The output from the analytical depletion functions is the estimated streamflow depletion in each stream segment caused by each well throughout the entire RRCA simulation period.

2.3.4 Comparison between analytical depletion functions and MODFLOW

To systematically assess different aspects of analytical depletion function performance, we calculated four fit metrics which are described below. To assess the drivers of analytical depletion function performance, we conducted a regional sensitivity analysis for each of the fit metrics in response to each of the well and landscape characteristics used to define the well sample (Figure 2; Section 2.3.1). The regional sensitivity analysis is meant to identify conditions under which the performance of analytical depletion functions exceeds a defined performance threshold (Spear and Hornberger 1980; Wagener et al. 2001; Pianosi et al. 2016), which we set separately for each of the four fit metrics:

1. *Spatial distribution of primary impact:* The percentage of pumping simulations in which the stream segment most affected by groundwater pumping matched between the analytical depletion functions and MODFLOW model. For regional sensitivity analysis, a threshold value of 50% was used to separate good (match ≥ 50%) from poor (match < 50%) performance.
2. *Magnitude of primary impact:* The mean absolute difference (MAD) between the volumetric depletion (*Qs*) in each stream segment predicted by the analytical depletion function and MODFLOW model, normalized to the range of predicted *Qs* values from

MODFLOW. The normalization allows for comparison across a range of depletion conditions - for instance, a difference in predicted Qs of 100 $m^3 d^{-1}$ is more problematic when actual Qs is 200 $m^3 d^{-1}$ than when actual Qs is 5000 $m^3 d^{-1}$. For regional sensitivity analysis, a threshold value of 0.25 was used to separate good (normalized MAD ≤ 0.25) from poor (normalized MAD > 0.25) performance. Note that we use the term MAD, rather than Mean Absolute Error, because differences between the MODFLOW model and analytical depletion functions may be caused by errors in either of the two approaches.

3. *Spatial distribution of overall impacts:* The Kling-Gupta Efficiency (KGE) between the volumetric depletion (*Qs*) in each stream segment predicted by the analytical depletion function and MODFLOW model. KGE is a hydrological performance indicator which accounts for differences in correlation, variability, and bias (Gupta et al. 2009; Kling et al. 2012). Similar to the Nash-Sutcliffe Efficiency, a KGE value of 1.0 indicates perfect agreement and lower values indicate worse agreement. As a benchmark, KGE > -0.41 indicates better agreement than simply using the mean (Knoben et al. 2019). For regional sensitivity analysis, a threshold value of -0.41 was used to separate good (KGE ≥ -0.41) from poor (KGE < -0.41) performance.
4. *Magnitude of overall impacts:* The bias between the total streamflow depletion across all segments for an individual well simulated by the analytical depletion function and the MODFLOW model, normalized to the range of predicted total streamflow depletion from MODFLOW. For regional sensitivity analysis, a threshold value of 75% was used to separate good (absolute bias ≤ 75%) from poor (absolute bias > 75%) performance.

This study focused on a comparison between the analytical depletion functions and the RRCA MODFLOW model because of the lack of large-scale streamflow depletion estimates. At the scale of an individual stream segment, analytical approaches can be evaluated via controlled field experiments (Hunt et al., 2001; Kollet & Zlotnik, 2003). However, at large spatial scales streamflow depletion is obscured by interannual variability in weather, lag times between pumping and depletion, and other management activities such as surface water withdrawals (Gleeson & Richter, 2018), and therefore calibrated numerical models are the preferred approach to quantify streamflow depletion (Barlow & Leake, 2012). Despite the limitations of the RRCA model (described in Section 2.1), the RRCA model was calibrated via comparison to historical baseflow data and therefore represents the best available estimates of streamflow depletion, and has been widely used for previous scientific studies (de Graaf et al., 2019; Hu et al., 2015, 2017; Ou et al., 2018). However, we acknowledge the potential for error in both the RRCA models and analytical depletion functions, and therefore our study focuses on agreement and differences between the two approaches.

3 Results and Discussion

3.1 Overall performance

Overall, we find a strong agreement between the analytical depletion functions and MODFLOW predictions of streamflow depletion. Variability among analytical depletion function formulations is explored in the following section. The best-performing analytical depletion function combined the adjacent+expanding stream proximity criteria, the web squared depletion apportionment equation, and the Glover analytical model, which agrees with the results from a previous comparison in the Navarro River Watershed (Zipper et al. 2019b).

There is strong agreement between this analytical depletion function and the MODFLOW model across our four performance criteria (Table 1). Over the final 20 years of the simulation period, the most-affected stream segment is identified correctly for 53.9% of pumping wells, the MAD of predicted depletion in the most-affected segment is 0.048 of the range in predicted depletion, the KGE of predicted depletion across all segments is 0.779, and the bias for predicted total streamflow depletion is 0.4%. Analytical depletion function is significantly better than using a standalone analytical model (without stream proximity criteria or depletion apportionment equations) for all metrics except the identification of the most affected stream segment (Table 1), highlighting the ability of analytical depletion functions to improve predictions for real-world settings compared to a standalone analytical model.

Identification of the most-affected segment is substantially lower than previous work, which was generally >70% correct in the Navarro River Watershed (Zipper et al. 2019b). Results from the standalone analytical model, which always used the stream segment closest to each well, had the same skill in identifying the most-affected segment (53.9%) which indicates that for 46.1% of wells the most-affected stream segment was not the closest stream segment to the well. This may be driven by the fact that well-stream distances and numerical model discretization are an order of magnitude larger in this domain compared to the Navarro River watershed, and therefore subsurface controls on flow such as spatial heterogeneity in T and S exert a stronger control over the distribution of pumping impacts.

Despite a negligible overall bias, this analytical depletion function tends to have a higher estimate than MODFLOW for both segment-resolution and total streamflow depletion at low magnitudes and a lower estimate at high magnitudes (Figure 3). The largest differences between MODFLOW and analytical depletion function estimates tend to be driven by a relatively small number of wells which are located near the edge of the domain, which is consistent for both segment-resolution and total streamflow depletion. The cluster of points in which the analytical depletion function produces substantially higher estimates of depletion compared to MODFLOW are associated with two wells on the southeastern margin of the domain that have several extreme characteristics relative to the overall well sample. These wells are the minimum possible distance from surface water cells given the model discretization (one grid cell, or 1.6 km) yet relatively far from evapotranspiration cells (>45 km, or 85th percentile among well sample), and also have very low transmissivity (~50 m^2 d^{-1}, or 6th percentile). In contrast, the points in which analytical depletion functions have the largest underestimate relative to MODFLOW are associated with two wells on the northern edge of the domain that are also extremely close to a stream (two grid cells, or 3.2 km) but have a very high transmissivity (~1900 m^2 d^{-1}, or 95th percentile).

The primary differences between segment-resolution streamflow depletion (Figure 3a) and total streamflow depletion caused by a well (Figure 3b) occur at low magnitudes of depletion. As discussed above, all points with high magnitudes of depletion tend to be very close to a surface water feature of some sort and therefore depletion is dominated by a single segment. In contrast, wells causing low levels of depletion tend to be far from stream segments and therefore depletion is distributed throughout more segments, but remains low even when the depletion is added together across all segments.

While there is variability in bias among analytical depletion functions (Table 1), none of the analytical depletion function formulations predict substantially higher depletion than the best-performing analytical depletion function (Figure S9 and Figure S10), indicating that the underestimate in depletion at high magnitudes (Figure 3) may be a persistent problem for analytical depletion functions in this setting. This finding is in contrast to the typical assumption that analytical approaches provide conservative estimates of streamflow depletion (Sophocleous et al. 1995; Rathfelder 2016) and may be problematic from a water management perspective because underestimating the depletion from the wells with the largest impacts could lead to an overallocation of water resources (Zipper et al. 2018a). As a result, analytical depletion functions should not be considered a “worst-case” estimate of depletion, but rather a minimally-biased estimate which may overestimate or underestimate depletion relative to the MODFLOW model.

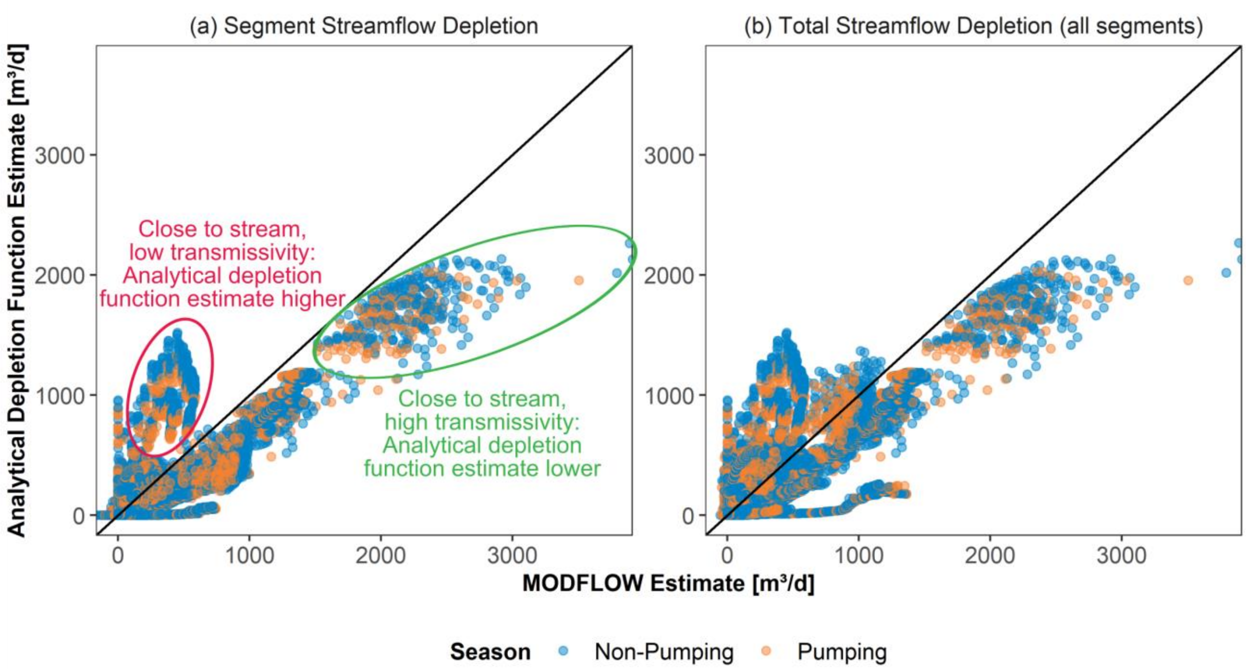

Figure 3. Comparison between analytical depletion function and MODFLOW predictions of (a) segment-scale streamflow depletion, (b) total streamflow depletion summed across all segments for a given well. Circles on depletion plot indicate 'higher estimate' and 'lower estimate' points discussed in Section 3.1 text.

Table 1. Analytical depletion function performance for different fit metrics, calculated for each month of simulations and averaged over the final 20 years of the simulations. All of the analytical depletion functions shown in this table used specific yield for the storage parameter and included DRN features.

Stream Proximity Criteria	Depletion Apportionment Equation	Spatial distribution of primary impact [% most-affected correct]	Magnitude of primary impact [MAD segment streamflow depletion, normalized]	Spatial distribution of overall impacts [KGE, segment streamflow depletion]	Magnitude of overall impacts [% bias, total streamflow depletion]
Adjacent	Inverse Distance	50.7	0.056	0.701	-8.0
Adjacent	Inverse Distance Squared	50.8	0.054	0.695	15.1
Adjacent	Web	**52.4***	**0.045***	0.699	-20.9
Adjacent	Web Squared	**53.9***	0.048	**0.767***	4.2
Adjacent + Expanding	Inverse Distance	50.0	0.057	0.697	-18.0
Adjacent + Expanding	Inverse Distance Squared	50.1	0.053	0.737	9.2
Adjacent + Expanding	Web	**52.5***	0.047	0.671	-26.5
Adjacent + Expanding	Web Squared	**53.9***	0.048	**0.779***	**0.4***
Analytical Only	Analytical Only	**53.9***	0.06	0.555	32.5

*Bold and starred values in each column indicate analytical depletion functions which are not significantly different from the best-performing function for that metric ($p > 0.05$ using Tukey's honest significant difference test).

3.2 Performance response to analytical depletion function formulation and input data

Analytical depletion formulation had relatively little impact on most of the model performance metrics. Comparing among stream proximity criteria, there is little difference between the Adjacent and Adjacent + Expanding stream proximity criteria (Table 1), likely due to the large size of the domain and relatively sparse stream network compared with Zipper et al. (2019b). Comparing among depletion apportionment equations, the inverse distance and inverse distance squared depletion apportionment equations do not perform the best for any of the fit metrics evaluated (Table 1) indicating that considering stream network geometry with the web and web squared improves performance, though differences between approaches are only a few percentage points. Notably, the web squared depletion apportionment equation performed the best at the spatial distribution of the overall impacts (regardless of stream proximity criteria used), demonstrating its effectiveness at identifying streamflow depletion across a stream network. The superior overall performance of the web squared depletion apportionment equation relative to the web equation is due to a negative bias for wells with high amounts of total streamflow depletion (Table 1; Figure S10). This is caused by the increased weight given to near-well stream segments in the web squared approach (Zipper et al. 2018a).

Both the magnitude of predicted depletion and the relationship between MODFLOW and analytical depletion functions varied as a function of the boundary condition used in the MODFLOW model. In general, the highest levels of depletion tended to be predicted for the constant head boundary, which runs along the north side of the model domain (Figure 2a), and analytical depletion function estimates of depletion were consistently lower than MODFLOW (Figure 4a). In contrast, predicted depletion from the stream package tended to be more evenly distributed with a mixture of overestimates and underestimates relative to the MODFLOW model (Figure 4b). Depletion from drain features (which are diffuse boundaries representing springs in this model; Figure 2a) was small, but analytical depletion functions had consistently higher estimates than MODFLOW (Figure 4c).

The differences in predicted depletion among these boundary conditions are likely driven by a combination of hydrostratigraphy and MODFLOW model design. First, the constant head boundaries are found along the north side of the model domain and this region has the highest estimated transmissivity (Figure 2a) due to more conductive sediments and a greater saturated thickness (RRCA 2003). These higher conductivity materials, along with the close proximity of some wells to the stream (discussed in Section 3.1), explains why the largest depletion estimates are found for the northern part of the domain along the constant head boundary. Second, MODFLOW uses a streambed conductance term to simulate potential low-conductivity streambed materials for stream and drain features but not for constant head boundaries. This streambed layer is not represented in the Glover analytical model we use in our analytical depletion functions. Use of an analytical model that includes streambed conductance, such as Hunt (1999), may improve agreement for stream and drain boundary conditions, but would cause further underestimation of depletion in constant head boundaries.

Since analytical models are not traditionally designed for use in diffuse discharge features such as the springs represented by the drain package, we also compare analytical depletion function performance with and without drain features (Figure S11). Removing drains had relatively small impacts on model performance, particularly at high levels of depletion. Overall, removing DRNs meant that estimates of depletion in DRN segments went to 0, and as a result estimates of depletion in some other boundary conditions increased (Figure S11). Removing DRN features from the analytical depletion functions had mixed impacts on our four performance metrics. When DRNs were excluded from analytical depletion function calculations, the identification of the most affected segments degraded (42.2%, compared to

53.9% when DRNs were included) and total streamflow depletion had a negative bias of -8.4% (compared to 0.4% with DRNs). However, normalized MAD of depletion for the most affected segment improved to 0.043 without DRNs (compared to 0.048 with DRNs) and KGE for depletion of all stream segments rose to 0.811 without DRNs (compared to 0.779 with DRNs).

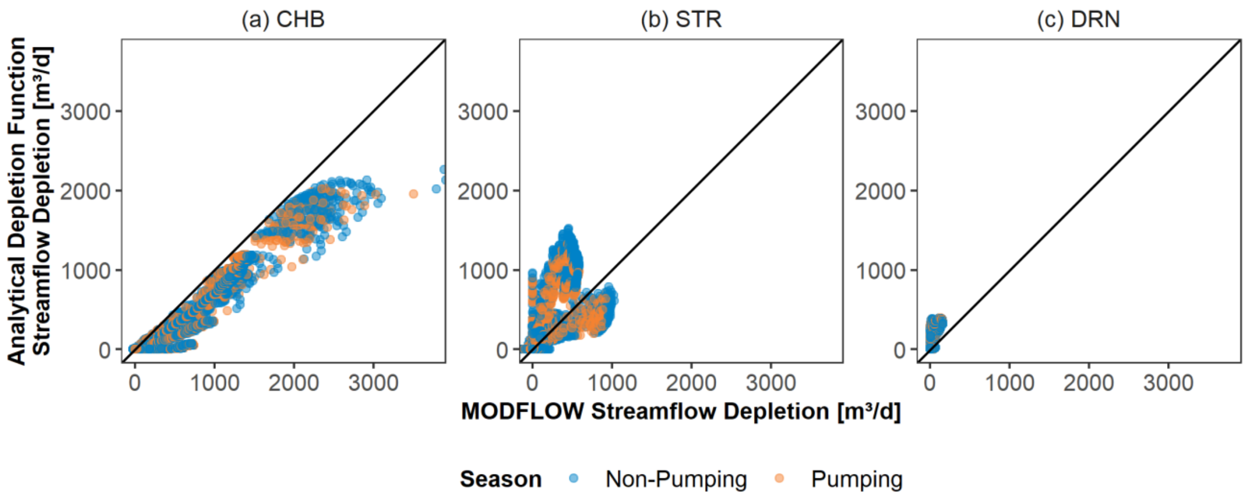

Figure 4. Comparison between analytical depletion function and MODFLOW predictions of segment-scale streamflow depletion for (a) constant head boundary package, (b) stream package, and (c) drain package in MODFLOW.

The storage parameter used in analytical depletion functions has a substantial impact on depletion predictions. While specific yield is typically used to represent storage in unconfined aquifers, the RRCA MODFLOW model uses a specific yield-based approximation of specific storage since the model assumes a constant transmissivity (details in Section 2.1). Recent work found that accurate estimates of specific yield are critical to obtain accurate estimates of groundwater depletion in the High Plains Aquifer, including parts of the RRCA domain (Butler et al. 2020). To assess the importance of using appropriate storage parameterizations in the analytical depletion functions, we compared our best-performing analytical depletion function in Table 1 (adjacent + expanding stream proximity criteria and web squared depletion apportionment equation) with both specific yield (as in Table 1) and specific storage as input. Using specific storage instead of specific yield led to substantially worse analytical depletion function performance for three of our performance metrics. Normalized MAD of depletion for the most affected segment rose to 0.130 with specific storage (compared to 0.048 with specific yield), KGE for depletion of all stream segments declined to -3.40 with specific storage (compared to 0.779 with specific yield), and percent bias for total streamflow depletion increased to 431% with specific storage (compared to 0.4% with specific yield).

The degradation in performance when analytical depletion functions use specific storage as input is primarily driven by a systematic overestimation of depletion relative to the MODFLOW model during the pumping season (Figure 5). This occurs because specific storage values in the RRCA MODFLOW model were defined by dividing specific storage by the saturated thickness, causing them to be 1-2 orders of magnitude lower than specific yield values. The lower specific storage values cause the streamflow depletion to occur much more quickly after the onset of pumping, and confirm the inappropriateness of using specific storage as input for analytical depletion functions in unconfined settings where specific yield is more appropriate. Combined, our analysis indicates that data collection efforts should prioritize high-accuracy estimates of transmissivity and storativity to improve accuracy of both streamflow depletion and groundwater depletion predictions, since hydraulic diffusivity (the ratio of storativity to transmissivity) is fundamental to the timing and magnitude of streamflow depletion (Barlow & Leake, 2012). In areas with high-quality water use and water level data, emerging data-driven approaches may be a valuable tool for improving storativity estimates (Whittemore et al. 2016; Butler et al. 2016).

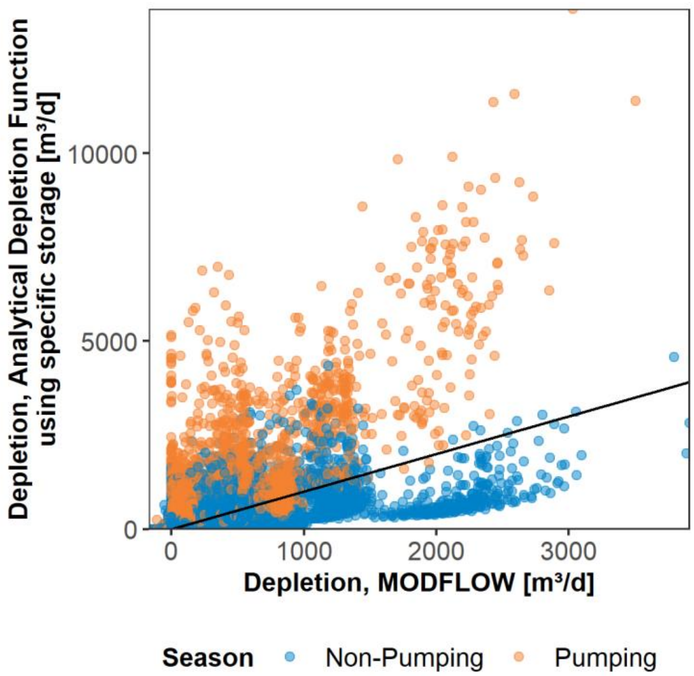

Figure 5. Comparison of predicted depletion from analytical depletion function using specific storage to MODFLOW estimates.

3.3 Well and landscape drivers of performance variability

Using the threshold defined in Section 2.3.4 for each performance metric, we found that 13 wells had good performance for all four metrics, 13 wells had good performance for three metrics, 33 wells had good performance for two metrics, 38 wells had good performance for a single metric, and 23 wells had good performance for no metrics. To investigate the relative importance of each parameter with comparable sample sizes, we compared wells with good performance in at least two fit metrics to wells with good performance in less than two fit metrics (Figure 6). Differences in the empirical cumulative distribution functions between the two samples for a given parameter indicates a potentially significant impact of that parameter on overall analytical depletion function performance (Wagener et al. 2001; Pianosi et al. 2016). Comparing across all fit metrics concurrently, the only two parameters that led to significant differences between these two samples were the hydrostratigraphic properties of transmissivity and specific storage. Wells tended to have better performance at intermediate to high values of transmissivity, agreeing with the observed drivers of over- and underestimated depletion (Figure 3). Specific storage has a strongly skewed relationship in our domain, but performance tended to be better when specific storage was higher.

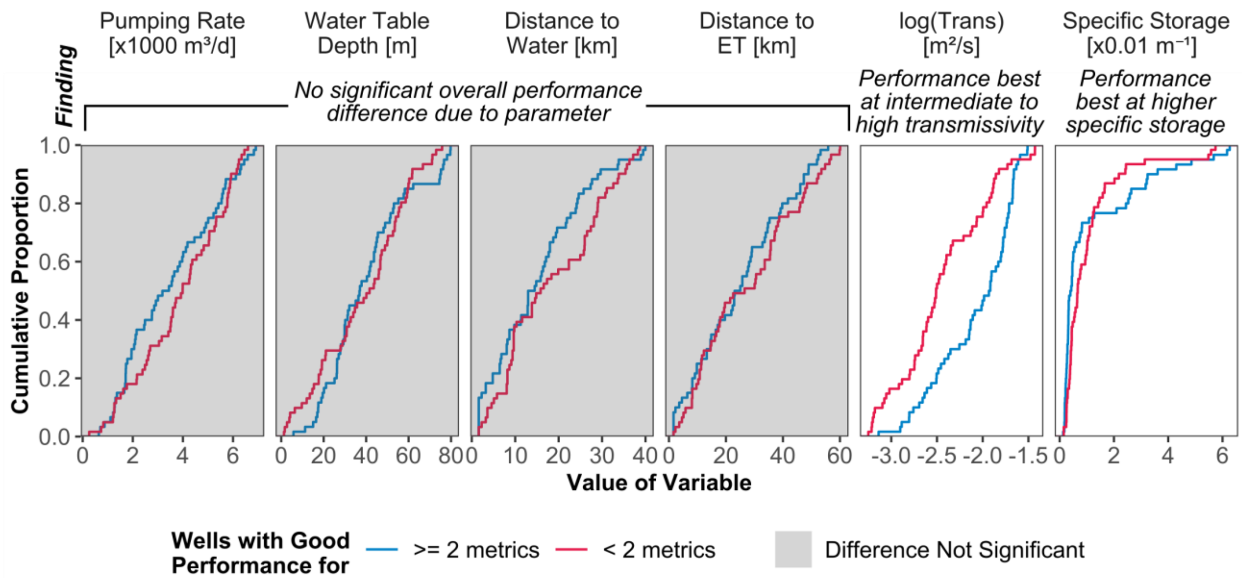

Figure 6. Regional sensitivity analysis results, expressed as empirical cumulative distribution functions for wells with good performance in at least two fit metrics and wells with good performance in less than 2 fit metrics. In shaded panels, distributions of the two samples are expected to be drawn from the same distribution (two-sample Kolmogorov-Smirnov test $p > 0.05$).

Investigating individual fit metrics, the regional sensitivity analysis found a significant impact of all of the well and landscape properties except pumping rate on at least one of the fit metrics, but no well or landscape property had a significant impact on all fit metrics (Figure 7). For pumping rate, none of the fit metrics differed significantly between wells with a good and poor fit, which supports the long-held assumption that streamflow response to pumping is independent of abstraction rate (Theis 1941; Glover and Balmer 1954; Hunt 1999). Transmissivity affected the most fit metrics, with intermediate transmissivity values associated with improved prediction of depletion (MAD in the most-affected segment and KGE in all segments) and bias. The difference between the ‘good’ and ‘poor’ wells at intermediate values of transmissivity further supports the observation that performance degrades in extremely high and low transmissivity settings near streams (Figure 3), and that variability in hydraulic conductivity is an important control over analytical depletion function accuracy (Sophocleous et al. 1995; Li et al. 2016). Unlike the overall assessment (Figure 6), looking at individual fit metrics revealed only a minor sensitivity to specific storage for one fit metric, the KGE of segment-resolution streamflow depletion, where good performing wells had a lower specific storage (Figure 7). The specific storage distribution across the domain is strongly skewed (Figure 2b), and the differences indicate that assessing the relative impact and importance of a given parameter depends on the aspect of model performance being considered.

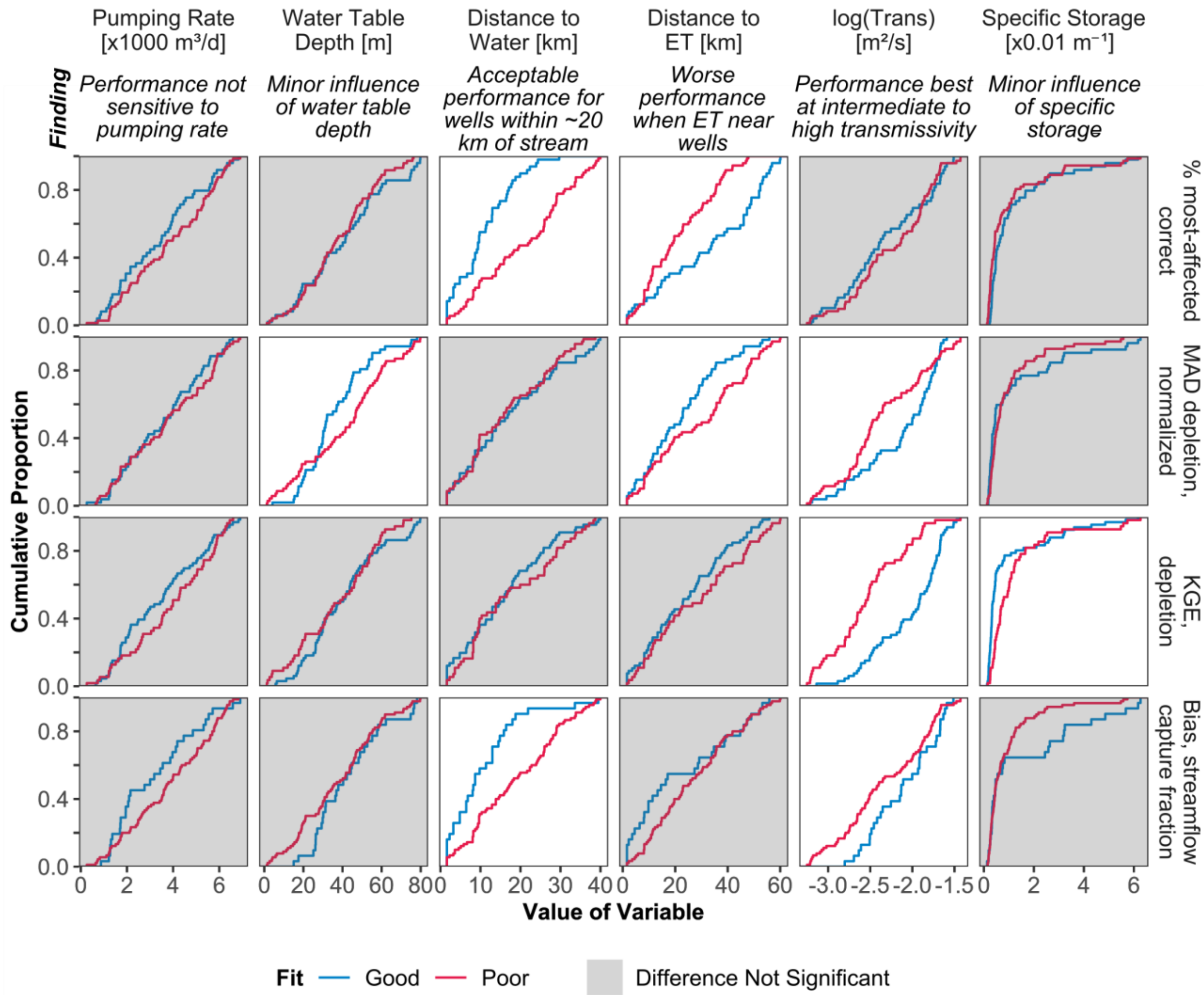

Figure 7. Regional sensitivity analysis results, expressed as empirical cumulative distribution functions for well characteristics for each performance criteria. In shaded panels, distributions of 'good' and 'poor' groups are expected to be drawn from the same distribution (two-sample Kolmogorov-Smirnov test $p > 0.05$).

There was an apparent threshold-type response as distance to the closest surface water feature increased; the identification of the most-affected segment and the total streamflow depletion bias both degraded significantly at distances greater than ~20 km. For distance to cells with ET, which is an alternate source of capture in the MODFLOW model that is not considered by the analytical depletion functions, wells that performed poorly for identifying the most-affected segment and MAD of depletion were primarily concentrated at shorter distances, while the MAD of depletion estimates improved at further distances to ET. Since phreatophytic ET is primarily concentrated along stream channels in the MODFLOW model (RRCA 2003), this indicates a spatial interplay between streamflow and ET capture sources which merits future investigation (Condon and Maxwell 2019). The water table depth had only a minor influence on the fit metrics, with better depletion predictions at intermediate water table depths (~20-50 m). It is important to note that we were assessing fit between the analytical depletion functions and the MODFLOW model, not agreement with field observations (which are not available). As a result, the division of fit into 'Good' and 'Poor' categories may be driven by errors in the MODFLOW model instead of or in addition to errors in the analytical depletion functions, and potential errors in the MODFLOW model may also vary in response to parameters evaluated here such as well-stream distance.

While we did not use the distance to the edge of the model domain as one of the variables guiding our well sample selection, we conducted a *post hoc* analysis to evaluate whether it had a significant impact on performance. We found that analytical depletion functions more successfully identify the most-affected segment and have an acceptable bias for wells that were closer to no-flow boundaries (Figure S12). This response is very similar to the observed influence of distance to the closest surface water feature (Figure 6) and we were not able to isolate the impacts of these no-flow boundaries because they are often co-located with or near surface water features (Figure 2). In aquifers of limited lateral extent, analytical models for bounded aquifers (Huang et al., 2018) may be useful methods to integrate into analytical depletion functions, but would need additional testing.

3.4 Synthesis with previous analytical depletion function evaluations

This work extends previous evaluations of analytical depletion functions by comparing their output to a calibrated numerical model in a highly stressed aquifer, a setting where analytical depletion functions have not previously been tested, and by systematically assessing the influence of well and hydrostratigraphic characteristics on results. Synthesizing across studies, we find general agreement that the adjacent + expanding stream proximity criteria and the web squared depletion apportionment equation produce the best agreement with numerical model output (Zipper et al. 2018a, 2019b). We also found performance was best when wells are close to streams, a finding that is consistent with previous work in coastal California (Zipper et al. 2019b) but in contrast to a study in British Columbia that found better agreement for wells further from streams (Li et al. 2020). We also extend this previous work by testing performance across 166 wells with a variety of pumping rates and demonstrated that performance is insensitive to pumping rate, indicating that analytical depletion functions are likely to be equally useful regardless of the magnitude of groundwater abstractions.

This study and previous work raise several key questions for further evaluation. First, we identify a potential spatial performance-related interaction between the distance from the well to the closest stream and closest ET cell (Figure 7). Additional testing is necessary to determine the conditions in which phreatophytic ET confounds analytical depletion function estimates of streamflow depletion (Condon and Maxwell 2019). Second, this and previous evaluations have focused on evaluation of a single well in isolation. While the current study investigates performance in the context of a heavily-stressed aquifer with many pumping wells, we isolated effects of an individual well by turning wells on/off one-at-a-time. While it is widely assumed that the output from analytical models is additive, work in the Republican River Watershed has shown this may not be the case (Schneider et al. 2017). For application of analytical depletion functions in heavily-stressed aquifers, systematic testing of cumulative impacts by evaluating the impacts of multiple wells concurrently is critical. Finally, recent field investigations found that analytical model performance in an urban setting varied as a function of stream stage (Flores et al. 2020), and will be important to test analytical depletion functions in a variety of stream stage conditions.

Given the low computational and data requirements of analytical depletion functions relative to numerical models, they may be a particularly valuable tool for applications requiring many streamflow depletion estimates under different conditions such as decision support tools, time series analysis, and simulation-optimization management modeling. Huggins et al. (2018) developed a workflow for integrating depletion apportionment equations and analytical models into existing web-based water decision support tools. Further, analytical depletion functions could be used to improve parameterization of pumping impacts in time series analysis approaches, which typically require a head response function that is often based on analytical methods (Bakker & Schaars, 2019; Obergfell et al., 2019; Shapoori et al., 2015). Finally, simulation-optimization models require the ability to test many different management approaches (Wagner, 1995; Singh, 2014). While this can be accomplished in relatively small domains using numerical models (Fienen et al., 2018), analytical depletion functions may complement other approaches such as metamodeling (Fienen et al., 2015) to provide estimates of streamflow depletion under diverse scenarios and identify optimal management solutions. For all of these potential applications, however, care should be taken to ensure that uncertainty and limitations of analytical approaches are appropriately considered, quantified, and shared with relevant stakeholders, so that decision-makers can determine whether the accuracy is sufficient for their needs.

4 Conclusions

Reliable estimates of streamflow depletion are critical for effective conjunctive management of groundwater and surface water resources. This study is the first systematic evaluation of analytical depletion functions for use in a heavily-stressed unconfined aquifer, and assesses how agreement between the numerical and analytical model varies as a function of well and hydrostratigraphic characteristics. We found that analytical depletion functions can produce similar estimates of streamflow depletion to an existing numerical model during both the pumping and non-pumping seasons, though they tend to over- or underestimate depletion relative to MODFLOW for wells very close to surface water features. Comparing among eight different analytical depletion functions, we found relatively little sensitivity to analytical depletion function formulation, but a strong response to the input storage parameter, indicating the critical importance of reliable parameter estimates. Among the analytical depletion functions, the one that performs most similarly to the numerical model included time-varying stream proximity criteria and a depletion apportionment equation that accounted for stream network geometry, which is consistent with previous studies. The analytical depletion function and numerical model are most similar for wells within ~20 km of a stream and intermediate values of transmissivity, with no sensitivity to pumping rate. These results do not suggest that numerical models should be replaced or superseded by analytical depletion functions, but rather that analytical depletion functions are a useful low-cost, low-effort approach to obtain comparable estimates of streamflow depletion in settings where calibrated numerical models are not available.

Acknowledgments and Data

Data and code are available at https://github.com/samzipper/RRCA-analytical during the review process and will be posted to a repository at the time of paper acceptance. We gratefully acknowledge the many people involved in the development of the Republican River Compact Administration MODFLOW model, which is available at http://www.republicanrivercompact.org/. This work was funded by a Natural Sciences and Engineering Research Council Collaborative Research and Development Grant (NSERC CRD) to the University of Victoria and Foundry Spatial. We also appreciate helpful feedback from the editor, associate editor, and three anonymous reviewers.

References

Ahlfeld DP, Schneider JC, Spalding CP (2016) Effects of nonlinear model response on allocation of streamflow depletion: exemplified by the case of Beaver Creek, USA. Hydrogeol J 24:1835–1845. https://doi.org/10.1007/s10040-016-1438-3

Bakker M, Post V, Langevin CD, et al (2016) Scripting MODFLOW Model Development Using Python and FloPy. Groundwater 54:733–739. https://doi.org/10.1111/gwat.12413

Bakker M, Post V, Langevin CD, et al (2018) FloPy. Version 3.29URL http://dx.doi.org/10.5066/F7BK19FH

Bakker M, Schaars F (2019) Solving Groundwater Flow Problems with Time Series Analysis: You May Not Even Need Another Model. Groundwater 57(6): 826–833. https://doi.org/10.1111/gwat.12927

Barlow PM, Leake SA (2012) Streamflow depletion by wells--Understanding and managing the effects of groundwater pumping on streamflow. U.S. Geological Survey, Reston VA

Barlow PM, Leake SA, Fienen MN (2018) Capture Versus Capture Zones: Clarifying Terminology Related to Sources of Water to Wells. Groundwater 56:694–704. https://doi.org/10.1111/gwat.12661

Beck HE, van Dijk AIJM, Miralles DG, et al (2013) Global patterns in base flow index and recession based on streamflow observations from 3394 catchments. Water Resour Res 49:7843–7863. https://doi.org/10.1002/2013WR013918

Bredehoeft JD (2002) The Water Budget Myth Revisited: Why Hydrogeologists Model. Ground Water 40:340–345. https://doi.org/10.1111/j.1745-6584.2002.tb02511.x

Bredehoeft JD, Papadopulos SS, Cooper HH (1982) Groundwater: The water budget myth. In:

Scientific Basis of Water Resource Management. National Research Council, Washington, D.C., pp 51–57
Butler JJ, Bohling GC, Whittemore DO, Wilson BB (2020) A roadblock on the path to aquifer sustainability: underestimating the impact of pumping reductions. Environ Res Lett 15:014003. https://doi.org/10.1088/1748-9326/ab6002
Butler JJ, Whittemore DO, Wilson BB, Bohling GC (2018) Sustainability of aquifers supporting irrigated agriculture: a case study of the High Plains aquifer in Kansas. Water International 43:815–828. https://doi.org/10.1080/02508060.2018.1515566
Butler JJ, Whittemore DO, Wilson BB, Bohling GC (2016) A new approach for assessing the future of aquifers supporting irrigated agriculture. Geophys Res Lett 43:2004–2010. https://doi.org/10.1002/2016GL067879
Butler JJ, Zhan X, Zlotnik VA (2007) Pumping-Induced Drawdown and Stream Depletion in a Leaky Aquifer System. Ground Water 45:178–186. https://doi.org/10.1111/j.1745-6584.2006.00272.x
Chen C, Liu L-M (1993) Joint Estimation of Model Parameters and Outlier Effects in Time Series. Journal of the American Statistical Association 88:284–297. https://doi.org/10.2307/2290724
Condon LE, Maxwell RM (2019) Simulating the sensitivity of evapotranspiration and streamflow to large-scale groundwater depletion. Science Advances 5:eaav4574. https://doi.org/10.1126/sciadv.aav4574
de Graaf IEM, Gleeson T, van Beek LPH, Sutanudjaja EH, Bierkens, MFP (2019). Environmental flow limits to global groundwater pumping. Nature, 574(7776), 90–94. https://doi.org/10.1038/s41586-019-1594-4
Deines JM, Kendall AD, Crowley MA, et al (2019) Mapping three decades of annual irrigation across the US High Plains Aquifer using Landsat and Google Earth Engine. Remote Sensing of Environment 233:111400. https://doi.org/10.1016/j.rse.2019.111400
Deines JM, Kendall AD, Hyndman DW (2017) Annual Irrigation Dynamics in the U.S. Northern High Plains Derived from Landsat Satellite Data. Geophysical Research Letters 44:9350–9360. https://doi.org/10.1002/2017GL074071
Feinstein DT, Fienen MN, Reeves HW, Langevin, CD (2016) A Semi-Structured MODFLOW-USG Model to Evaluate Local Water Sources to Wells for Decision Support. Groundwater 54(4):532–544. https://doi.org/10.1111/gwat.12389
Fienen MN, Bradbury KR, Kniffin M, Barlow PM (2018) Depletion Mapping and Constrained Optimization to Support Managing Groundwater Extraction. Groundwater 56:18–31. https://doi.org/10.1111/gwat.12536
Fienen MN, Nolan BT, Feinstein DT (2016) Evaluating the sources of water to wells: Three techniques for metamodeling of a groundwater flow model. Environmental Modelling & Software 77:95–107. https://doi.org/10.1016/j.envsoft.2015.11.023
Fienen MN, Nolan BT, Feinstein DT, Starn JJ (2015) Metamodels to Bridge the Gap Between Modeling and Decision Support. Groundwater 53:511–512. https://doi.org/10.1111/gwat.12339
Flores L, Bailey RT, Kraeger-Rovey C (2020) Analyzing the Effects of Groundwater Pumping on an Urban Stream-Aquifer System. JAWRA Journal of the American Water Resources Association. https://doi.org/10.1111/1752-1688.12827
Gleeson, T., & Richter, B. (2018). How much groundwater can we pump and protect environmental flows through time? Presumptive standards for conjunctive management

of aquifers and rivers. River Research and Applications, 34(1), 83–92. https://doi.org/10.1002/rra.3185
Glover RE, Balmer GG (1954) River depletion resulting from pumping a well near a river. Eos Trans AGU 35:468–470. https://doi.org/10.1029/TR035i003p00468
Gupta HV, Kling H, Yilmaz KK, Martinez GF (2009) Decomposition of the mean squared error and NSE performance criteria: Implications for improving hydrological modelling. Journal of Hydrology 377:80–91. https://doi.org/10.1016/j.jhydrol.2009.08.003
Haacker EMK, Kendall AD, Hyndman DW (2016) Water Level Declines in the High Plains Aquifer: Predevelopment to Resource Senescence. Groundwater 54:231–242. https://doi.org/10.1111/gwat.12350
Hamilton DA, Seelbach PW (2011) Michigan's water withdrawal assessment process and internet screening tool. Fisheries Division Special Report 55:
Harbaugh AW, Banta ER, Hill MC, McDonald MG (2000) MODFLOW-2000, The U.S. Geological Survey Modular Ground-Water Model - User Guide to Modularization Concepts and the Ground-Water Flow Process. U.S. Geological Survey
Hu, Y., Cai, X., & DuPont, B. (2015). Design of a web-based application of the coupled multi-agent system model and environmental model for watershed management analysis using Hadoop. Environmental Modelling & Software, 70, 149–162. https://doi.org/10.1016/j.envsoft.2015.04.011
Hu, Y., Quinn, C. J., Cai, X., & Garfinkle, N. W. (2017). Combining human and machine intelligence to derive agents' behavioral rules for groundwater irrigation. Advances in Water Resources, 109, 29–40. https://doi.org/10.1016/j.advwatres.2017.08.009
Huang C-S, Yang T, Yeh H-D (2018) Review of analytical models to stream depletion induced by pumping: Guide to model selection. Journal of Hydrology 561:277–285. https://doi.org/10.1016/j.jhydrol.2018.04.015
Huggins X, Gleeson T, Eckstrand H, Kerr B (2018) Streamflow Depletion Modeling: Methods for an Adaptable and Conjunctive Water Management Decision Support Tool. JAWRA Journal of the American Water Resources Association 54(5): 1024–1038. https://doi.org/10.1111/1752-1688.12659
Hunt B (1999) Unsteady Stream Depletion from Ground Water Pumping. Ground Water 37:98–102. https://doi.org/10.1111/j.1745-6584.1999.tb00962.x
Hunt, B., Weir, J., & Clausen, B. (2001). A Stream Depletion Field Experiment. Ground Water, 39(2), 283–289. https://doi.org/10.1111/j.1745-6584.2001.tb02310.x
Jenkins CT (1968) Techniques for Computing Rate and Volume of Stream Depletion by Wells. Ground Water 6:37–46. https://doi.org/10.1111/j.1745-6584.1968.tb01641.x
Khan HF, Brown CM (2019) Effect of Hydrogeologic and Climatic Variability on Performance of a Groundwater Market. Water Resources Research 55:4304–4321. https://doi.org/10.1029/2018WR024180
Kling H, Fuchs M, Paulin M (2012) Runoff conditions in the upper Danube basin under an ensemble of climate change scenarios. Journal of Hydrology 424–425:264–277. https://doi.org/10.1016/j.jhydrol.2012.01.011
Knoben WJM, Freer JE, Woods RA (2019) Technical note: Inherent benchmark or not? Comparing Nash–Sutcliffe and Kling–Gupta efficiency scores. Hydrology and Earth System Sciences 23:4323–4331. https://doi.org/10.5194/hess-23-4323-2019
Kollet SJ & Zlotnik VA (2003). Stream depletion predictions using pumping test data from a heterogeneous stream–aquifer system (a case study from the Great Plains, USA). Journal

of Hydrology, 281(1), 96–114. https://doi.org/10.1016/S0022-1694(03)00203-8
Kollet SJ, Zlotnik VA, & Ledder G (2002) "A Stream Depletion Field Experiment," by Bruce Hunt, Julian Weir, and Bente Clausen. Ground Water 40(4): 448–449. https://doi.org/10.1111/j.1745-6584.2002.tb02523.x
Larsen LG, Woelfle-Erskine C (2018) Groundwater Is Key to Salmonid Persistence and Recruitment in Intermittent Mediterranean-Climate Streams. Water Resources Research 54:8909–8930. https://doi.org/10.1029/2018WR023324
Li B-D, Sampath PV, Liao H (2016) A study on the hydro-geologic factors that affect streamflow depletion. Hydrological Sciences Journal 61:2133–2143. https://doi.org/10.1080/02626667.2015.1083649
Li Q, Zipper SC, Gleeson T (2020) Analytical Depletion Functions and Response Time of Groundwater Pumping Impacts on Environmental Flows. British Columbia Ministry of Environment and Climate Change Strategy, Victoria BC
López-de-Lacalle J (2019) tsoutliers: Detection of Outliers in Time Series. Version R package version 0.6-8URL https://CRAN.R-project.org/package=tsoutliers
McDonald MG, Harbaugh AW (1988) A modular three-dimensional finite-difference ground-water flow model. U.S. Geological Survey
McKay MD, Beckman RJ, Conover WJ (1979) A Comparison of Three Methods for Selecting Values of Input Variables in the Analysis of Output from a Computer Code. Technometrics 21:239–245. https://doi.org/10.2307/1268522
Obergfell C, Bakker M, Maas K (2019) Identification and Explanation of a Change in the Groundwater Regime using Time Series Analysis. Groundwater 57(6): 886–894. https://doi.org/10.1111/gwat.12891
Ou, G., Munoz-Arriola, F., Uden, D. R., Martin, D., Allen, C. R., & Shank, N. (2018). Climate change implications for irrigation and groundwater in the Republican River Basin, USA. Climatic Change, 151(2), 303–316. https://doi.org/10.1007/s10584-018-2278-z
Pianosi F, Beven K, Freer J, et al (2016) Sensitivity analysis of environmental models: A systematic review with practical workflow. Environmental Modelling & Software 79:214–232. https://doi.org/10.1016/j.envsoft.2016.02.008
Rathfelder KM (2016) Modelling tools for estimating effects of groundwater pumping on surface waters. Ministry of Environment, Province of B.C.
Reeves HW, Hamilton DA, Seelbach PW, Asher AJ (2009) Ground-water-withdrawal component of the Michigan water-withdrawal screening tool. U.S. Geological Survey, Reston VA
Rohde MM, Froend R, Howard J (2017) A Global Synthesis of Managing Groundwater Dependent Ecosystems Under Sustainable Groundwater Policy. Groundwater n/a-n/a. https://doi.org/10.1111/gwat.12511
RRCA (2003) Republican River Compact Administration Ground Water Model
RRCA (2005) Republican River Compact Administration Groundwater Model User Manual (DRAFT) V12s 1.0. Republican River Compact Administration
Schneider JC, Ahlfeld DP, Spalding CP (2017) Allocation of Streamflow Depletion Impacts under Nonlinear Conditions. JAWRA Journal of the American Water Resources Association 53:697–706. https://doi.org/10.1111/1752-1688.12525
Shapoori V, Peterson TJ, Western AW, Costelloe JF (2015) Top-down groundwater hydrograph time-series modeling for climate-pumping decomposition. Hydrogeology Journal 23(4): 819–836. https://doi.org/10.1007/s10040-014-1223-0

Singh A (2014) Simulation–optimization modeling for conjunctive water use management. Agricultural Water Management 141: 23–29. https://doi.org/10.1016/j.agwat.2014.04.003

Singh SK (2009) Flow Depletion Induced by Pumping Well from Stream Perpendicularly Intersecting Impermeable/Recharge Boundary. Journal of Irrigation and Drainage Engineering 135:499–504. https://doi.org/10.1061/(ASCE)IR.1943-4774.0000095

Sophocleous M, Koussis A, Martin JL, Perkins SP (1995) Evaluation of Simplified Stream-Aquifer Depletion Models for Water Rights Administration. Ground Water 33:579–588. https://doi.org/10.1111/j.1745-6584.1995.tb00313.x

Spear RC, Hornberger GM (1980) Eutrophication in Peel Inlet—II. Identification of critical uncertainties via generalized sensitivity analysis. Water Research 14:43–49. https://doi.org/10.1016/0043-1354(80)90040-8

Theis CV (1941) The effect of a well on the flow of a nearby stream. Eos Trans AGU 22:734–738. https://doi.org/10.1029/TR022i003p00734

Wagener T, Boyle DP, Lees MJ, et al (2001) A framework for development and application of hydrological models. Hydrology and Earth System Sciences 5:13–26. https://doi.org/10.5194/hess-5-13-2001

Whittemore DO, Butler JJ, Wilson BB (2016) Assessing the major drivers of water-level declines: new insights into the future of heavily stressed aquifers. Hydrol Sci J-J Sci Hydrol 61:134–145. https://doi.org/10.1080/02626667.2014.959958

Yeh H-D, Chang Y-C, Zlotnik VA (2008) Stream depletion rate and volume from groundwater pumping in wedge-shape aquifers. Journal of Hydrology 349:501–511. https://doi.org/10.1016/j.jhydrol.2007.11.025

Zipper SC, Carah JK, Dillis C, et al (2019a) Cannabis and residential groundwater pumping impacts on streamflow and ecosystems in Northern California. Environ Res Commun 1:125005. https://doi.org/10.1088/2515-7620/ab534d

Zipper SC, Dallemagne T, Gleeson T, et al (2018a) Groundwater pumping impacts on real stream networks: Testing the performance of simple management tools. Water Resources Research 54:5471–5486. https://doi.org/10.1029/2018WR022707

Zipper SC, Gleeson T, Kerr B, et al (2019b) Rapid and Accurate Estimates of Streamflow Depletion Caused by Groundwater Pumping Using Analytical Depletion Functions. Water Resources Research 55:5807–5829. https://doi.org/10.1029/2018WR024403

Zipper SC, Lamontagne-Hallé P, McKenzie JM, Rocha AV (2018b) Groundwater controls on post-fire permafrost thaw: Water and energy balance effects. Journal of Geophysical Research: Earth Surface 123:2677–2694. https://doi.org/10.1029/2018JF004611

Zlotnik VA, Tartakovsky DM (2008) Stream Depletion by Groundwater Pumping in Leaky Aquifers. Journal of Hydrologic Engineering 13:43–50. https://doi.org/10.1061/(ASCE)1084-0699(2008)13:2(43)

Supplemental Information

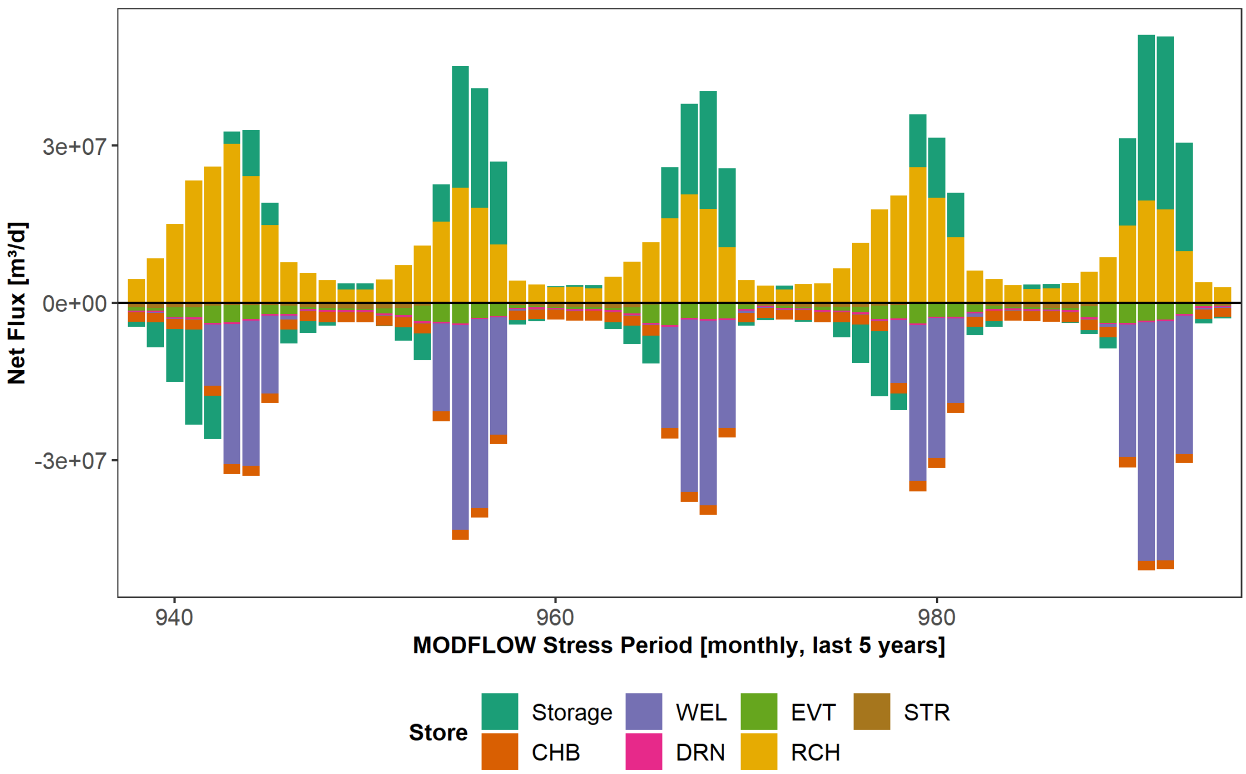

Figure S1. Net water budget for baseline RRCA MODFLOW model over last 5 years of simulation. The black line which is indistinguishable from 0 is the net error (inflow - outflows) at each timestep.

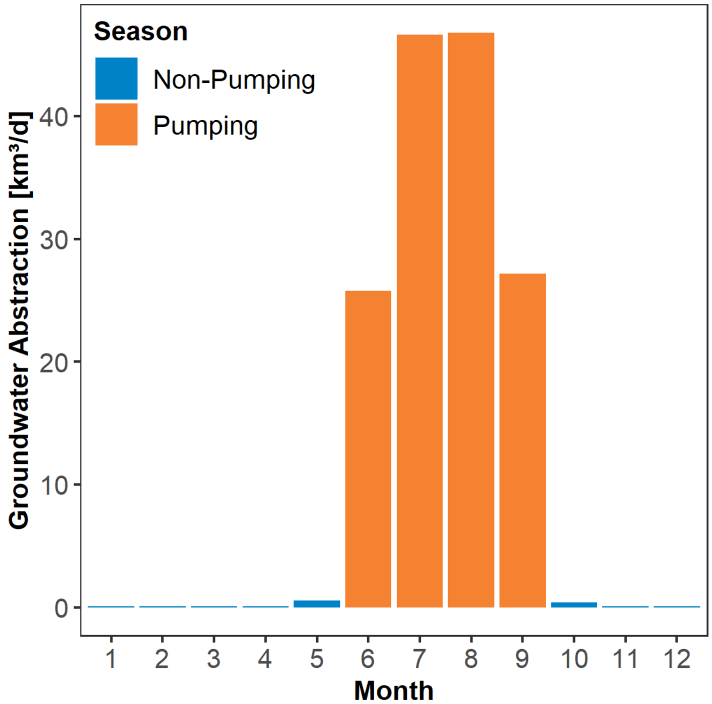

Figure S2. Monthly total pumping by all wells within MODFLOW model domain for the final year of simulation, showing division of year into Pumping Season (June-September) and Non-Pumping Season (all other months).

Figure S3. Monthly pumping schedule for each of the 166 wells included in well sample for last 5 years of simulation.

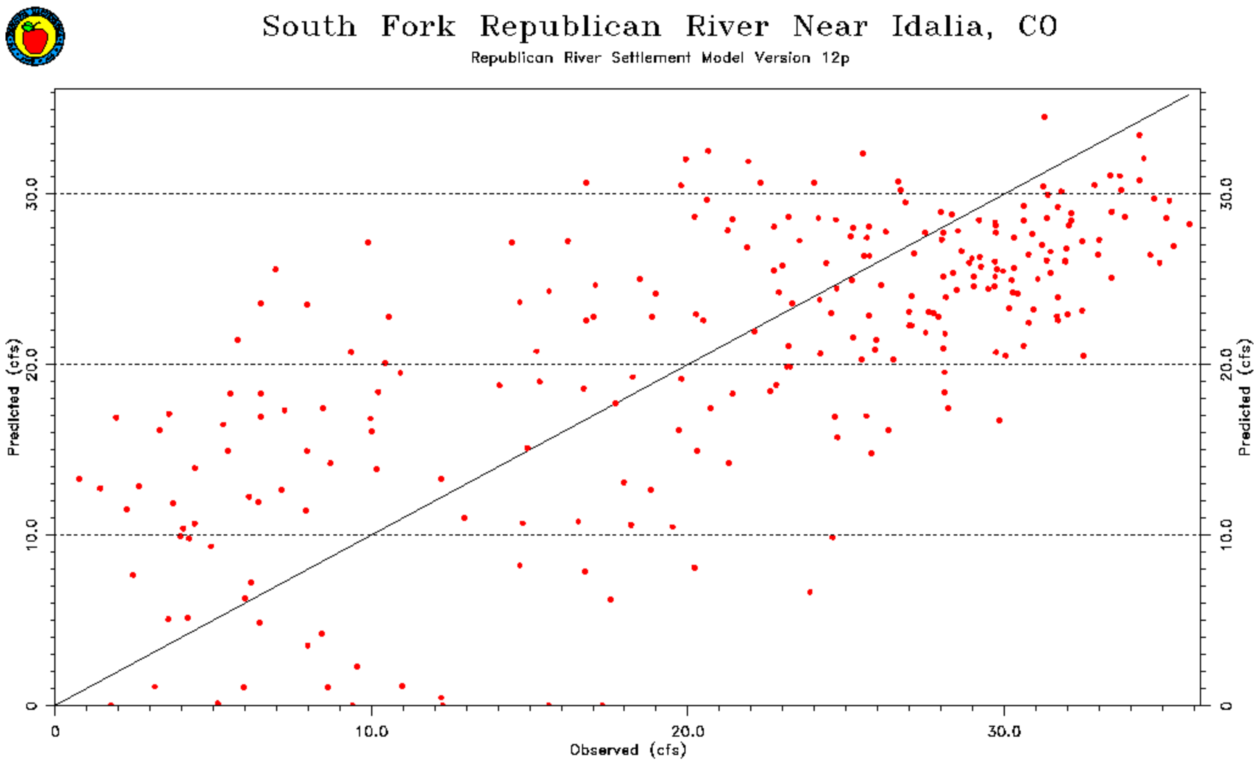

Figure S4. RRCA model calibration from the South Fork Republican River near Idalia CO, which is the furthest point upstream for which calibration results are available. Source: https://www.republicanrivercompact.org/v12p/html/bf/05c.html

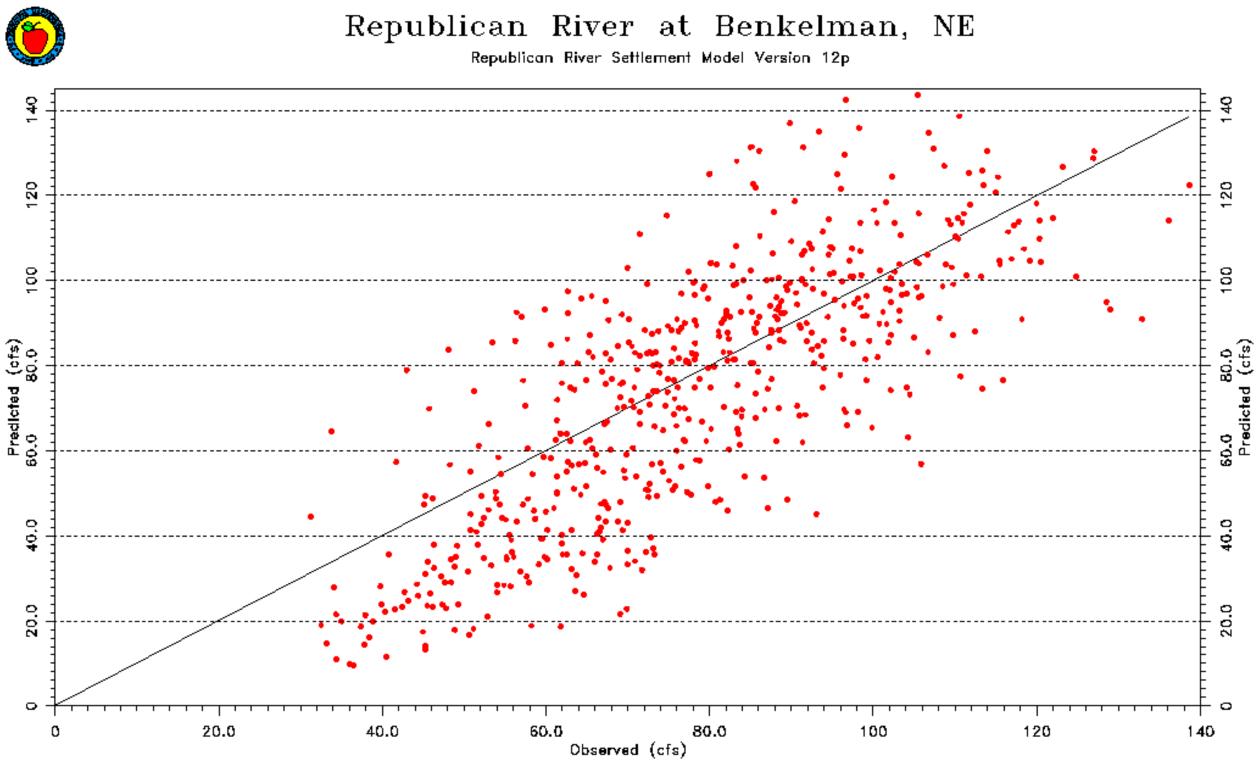

Figure S5. RRCA model calibration from Republican River at Benkelman NE, which is between Idalia CO and Hardy NE. Source: https://www.republicanrivercompact.org/v12p/html/bf/45c.html

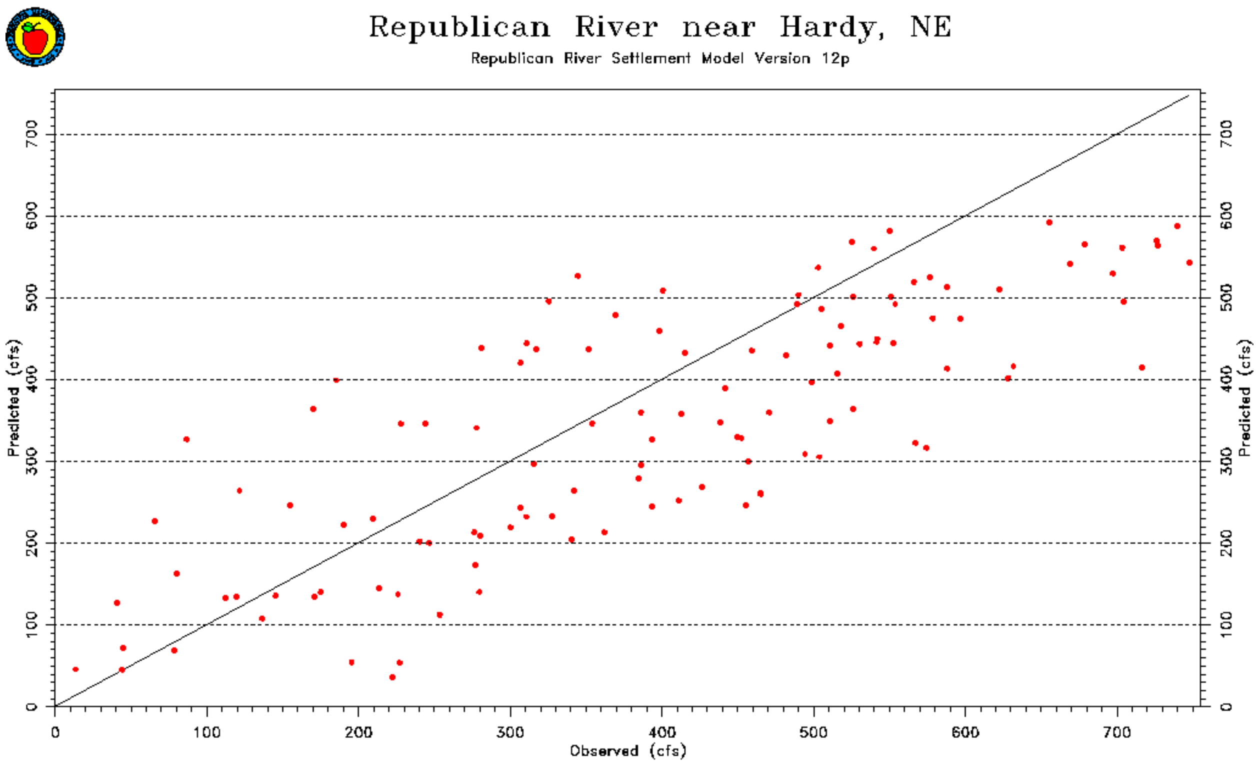

Figure S6. RRCA predicted baseflow vs. observed baseflow from the Republican River near Hardy NE, which is the furthest downstream point for which calibration results are available. Source: https://www.republicanrivercompact.org/v12p/html/bf/48c.html

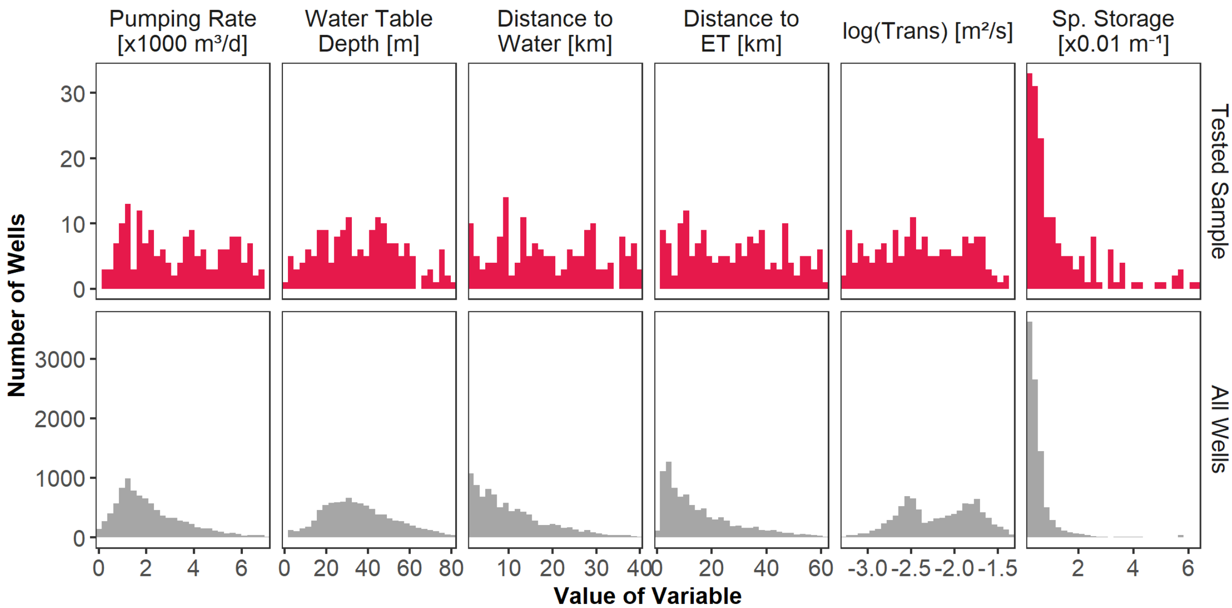

Figure S7. (top row) Properties of wells selected for model experiments, identical to Figure 2b. (bottom row) Properties of all wells in model domain.

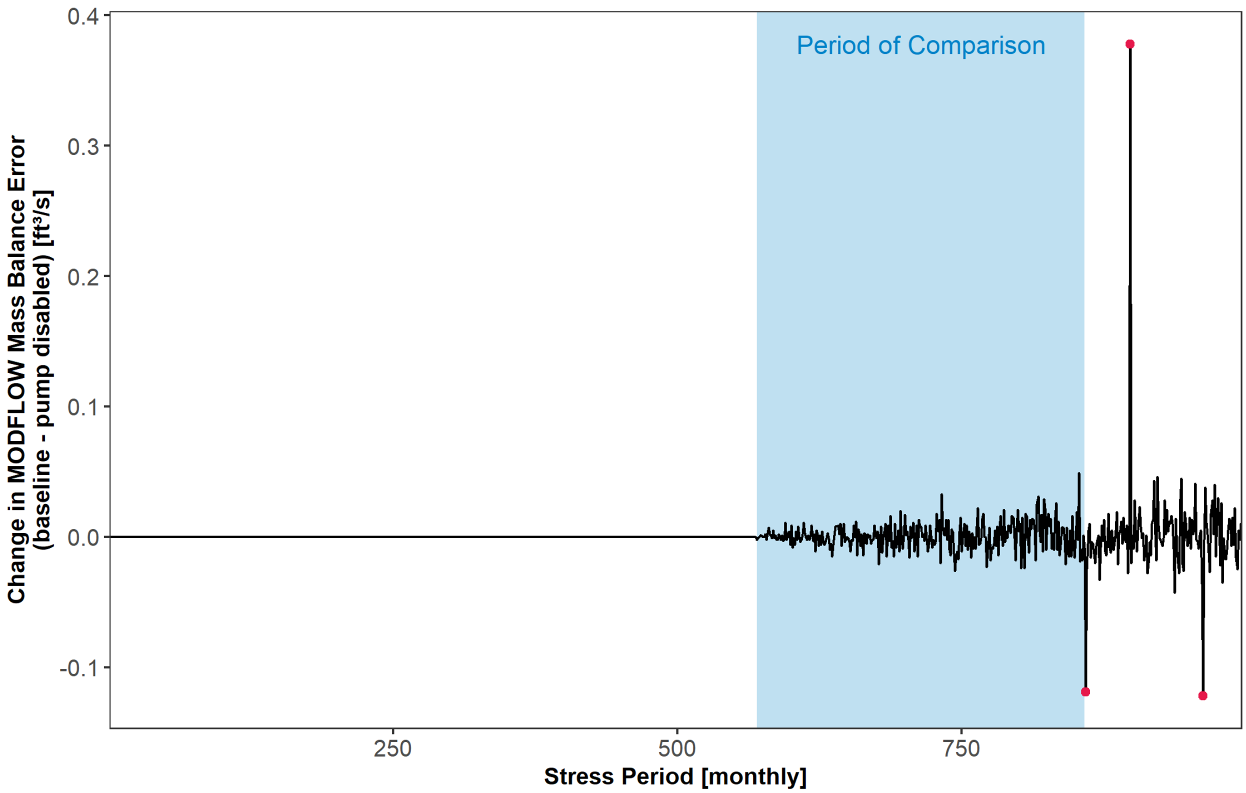

Figure S8. Demonstration of selection of period of comparison for a well, shown as shaded blue background. The period of comparison begins at the onset of pumping and ends at the timestep prior to the first detected outlier. The red dots indicate outliers in the timeseries of mass balance change.

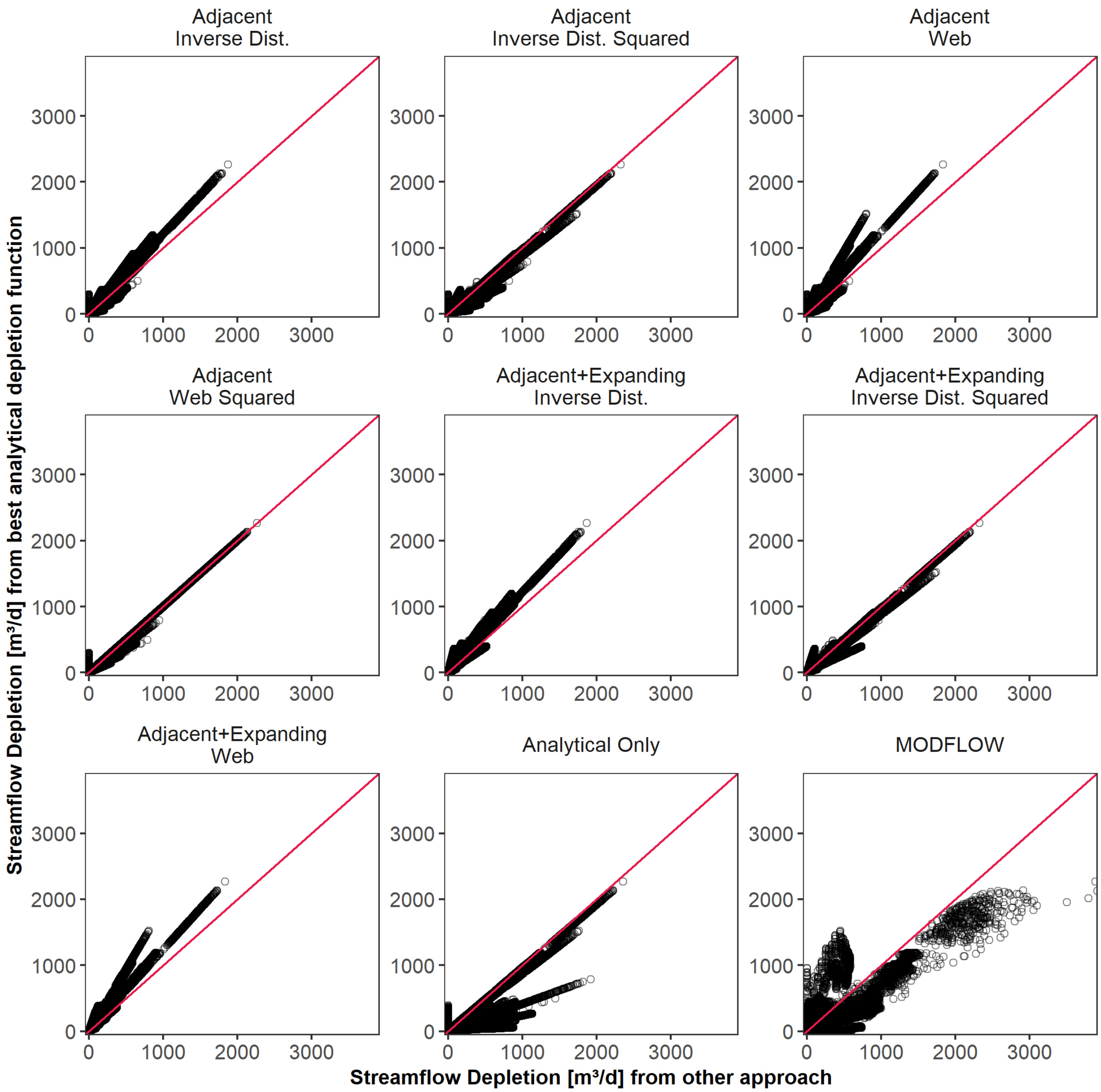

Figure S9. Comparison between segment streamflow depletion predicted by the best-performing analytical depletion function, which uses the adjacent+expanding stream proximity criteria and web squared depletion apportionment equation (Table 1), and all other analytical depletion functions, analytical model only, and MODFLOW model. Each point shows the streamflow depletion at a single timestep for the response of one stream segment to a single well. Red lines show 1:1 relationship.

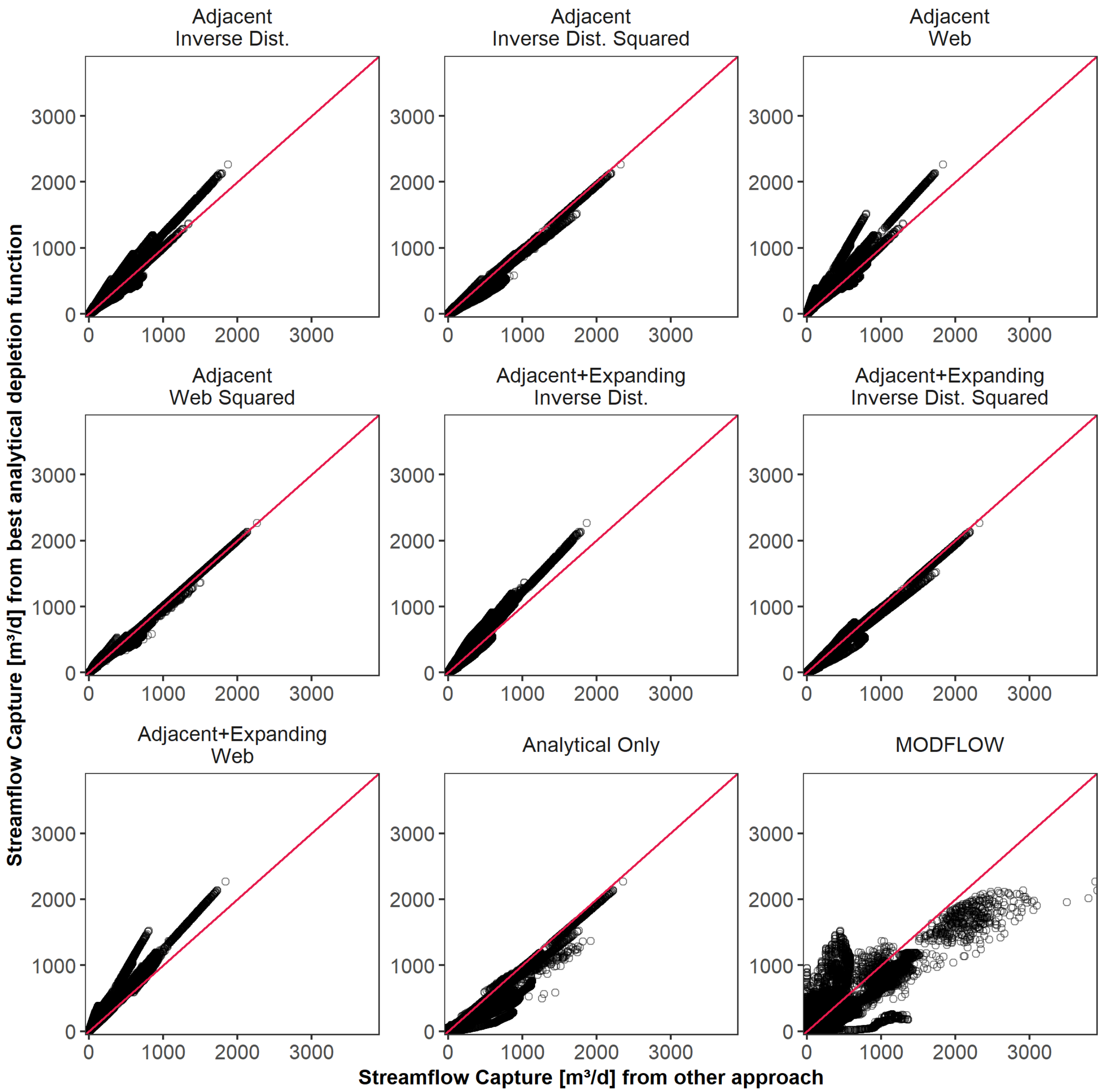

Figure S10. Comparison between total streamflow depletion predicted by the best-performing analytical depletion function, which uses the adjacent+expanding stream proximity criteria and web squared depletion apportionment equation (Table 1), and all other analytical depletion functions, analytical model only, and MODFLOW model. Each point shows the total streamflow depletion summer across all segments at a single timestep for a single well. Red lines show 1:1 relationship.

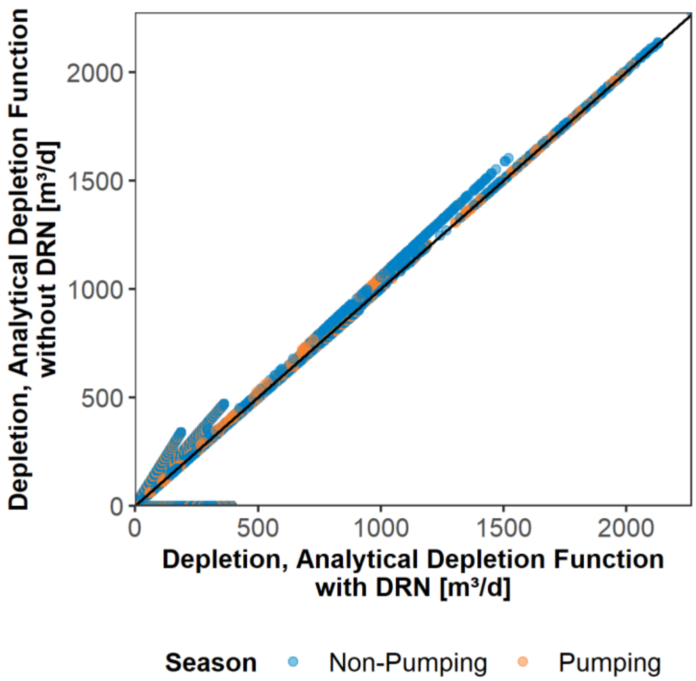

Figure S11. Depletion predicted by analytical depletion function with and without DRN features.

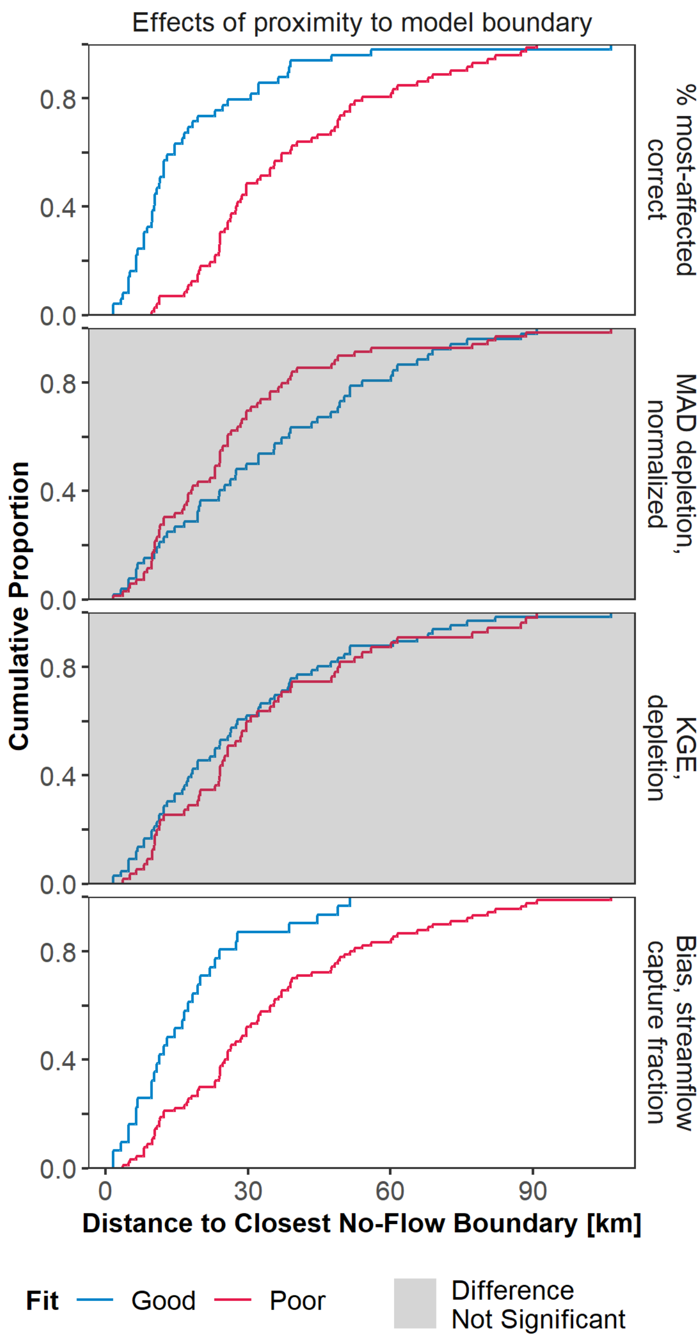

984
985 **Figure S12.** Regional sensitivity analysis of performance as a function of distance to the closest
986 no-flow cell. As in Figure 6, each plot is an empirical cumulative distribution functions for all
987 wells with respect to each performance criteria. In shaded panels, distributions of 'good' and
988 'poor' groups are expected to be drawn from the same distribution (two-sample Kolmogorov-
989 Smirnov test $p > 0.05$).